

ANALYSIS OF A SPACE-TIME UNFITTED FINITE ELEMENT METHOD FOR PDES ON EVOLVING SURFACES

ARNOLD REUSKEN* AND HAUKE SASS†

Abstract. In this paper we analyze a space-time unfitted finite element method for the discretization of scalar surface partial differential equations on evolving surfaces. For higher order approximations of the evolving surface we use the technique of (iso)parametric mappings for which a level set representation of the evolving surface is essential. We derive basic results in which certain geometric characteristics of the exact space-time surface are related to corresponding ones of the numerical surface approximation. These results are used in an error analysis of a higher order space-time TraceFEM.

Key words. surface partial differential equation, space-time finite element method, CutFEM, TraceFEM, finite element error analysis

1. Introduction. In the past two decades a large toolbox of finite element methods for solving *scalar* partial differential equations (PDEs) on *evolving* surfaces has been developed. The probably most prominent method is the evolving surface finite element method (ESFEM) [4, 5, 14]. This is an elegant and popular method for which a complete error analysis has been developed [6, 5]. A key feature of this method is that it is based on a Lagrangian approach in which a triangulation of the initial surface and a corresponding finite element space are transported along the flow lines of a (given) velocity field. This makes the method attractive for problems with smoothly and slowly varying surfaces. There are also recent contributions [25, 15] in which the ESFEM is applied to problems with geometric singularities (e.g. droplet pinch-off). It is, however, well-known that such Lagrangian techniques have drawbacks if the geometry of the surface is strongly varying on the relevant time scales or if there are topological singularities, e.g., merging or splitting phenomena. Another finite element technique for PDEs on evolving surfaces is introduced in [17]. This method is based on an Eulerian approach in which the stabilized trace finite element method (TraceFEM) is used for spatial discretization and combined with standard finite differences (BDF) for the time discretization. With such an Eulerian approach it is easier to handle topological singularities. Furthermore, if the surface PDE is coupled with a bulk PDE, the use of TraceFEM, which is based on standard bulk finite element spaces, may lead to advantages concerning the implementation. In [17] an error analysis of this method is presented for BDF1 combined with higher order finite elements for spatial discretization. In this analysis geometry errors are treated but there is an issue concerning sufficiently accurate numerical integration on the approximate surface [17, Remark 4.1]. Yet another approach, also of Eulerian type, has been introduced in [20, 19] and uses the TraceFEM or CutFEM principle not only in space but in space-time. In other words, the discretization of the evolving surface PDE uses a restriction to the space-time surface of standard space-time finite element spaces on a fixed bulk (tensor product) space-time mesh. In the framework of CutFEM this is a natural approach for this class of partial differential equations. The structure of this space-time TraceFEM is such that it naturally fits to a level set representation of

*Institut für Geometrie und Praktische Mathematik, RWTH-Aachen University, D-52056 Aachen, Germany; email: reusken@igpm.rwth-aachen.de

†Institut für Geometrie und Praktische Mathematik, RWTH-Aachen University, D-52056 Aachen, Germany; email: sass@igpm.rwth-aachen.de

the evolving surface. Such level set representations are often used for problems with strongly varying surface geometries or with topological singularities.

In this paper we treat this space-time TraceFEM. Its main characteristics are the following. The method is of Eulerian type, using a (per time step) fixed unfitted bulk spatial triangulation and corresponding standard space-time (tensor product) finite element spaces. As input for the method one needs a level set representation of the evolving surface. If a sufficiently accurate (made precise further on in the paper) level set function approximation is available and higher order bulk space-time finite element spaces are used, the resulting surface PDE discretization method is also of (optimal) higher order accuracy for smoothly varying surfaces with sufficiently smooth solutions. Without any modifications the method can also be used for the discretization of problems with topological singularities. Of course, in such singular cases one can not expect global higher order convergence. In [20, 19] the method was introduced for piecewise linears (in space and time) and the issue of geometry approximation was not considered. In the recent paper [23] the method was extended in two directions. Firstly, a higher order variant was introduced based on the parametric TraceFEM [16]. Secondly, the so-called volume normal derivative stabilization was included. This stabilization is important, in particular for higher order finite elements, to control the conditioning of the resulting stiffness matrix. In [23] these extensions are explained and a systematic numerical study of this method is presented that demonstrates (optimal) higher order accuracy for smoothly varying surfaces with sufficiently smooth solutions and its robustness with respect to topological singularities.

An important topic of the present paper is an error analysis of this higher order space-time TraceFEM. We put the analysis in a rather general framework in the following sense. We assume that the evolving surface is characterized using a level set function $\phi = \phi(\mathbf{x}, t)$, $\mathbf{x} \in \Omega \subset \mathbb{R}^3$, $t \in [0, T]$. The smooth space-time surface, denoted by $S \subset \mathbb{R}^4$, is the zero level of $\phi(\cdot, t)$ for $t \in [0, T]$. For an efficient construction of a (higher order) approximation S_h of S we use the general technique of level set based parametric mappings. In [16] this technique is introduced for the case of a stationary surface and in [12] its generalization to space-time surfaces is treated.

In the first part of this paper we derive basic properties of this space-time surface approximation. More specifically, we examine relations between surface measures on S_h and S , derive useful integral transformation and partial integration formulas on S_h mirroring those on S , and show how to transform the space-time surface gradient of a function on S to the space-time surface gradient on S_h of an extension of this function. We also derive estimates on the change in surface measure when moving from S to S_h and on the size of conormal jumps in the (not necessarily shape regular) surface triangulation of S_h . For these geometric estimates we use results that are presented in the recent work [11]

The results of the first part of the paper, which depend essentially only on the level set function approximation $\phi_h \approx \phi$ and on properties of the space-time parametric mapping [12, 11], may be useful also in the development and analysis of methods other than space-time TraceFEM. In the second part of the paper we give an error analysis of the space-time TraceFEM introduced in [23]. In this analysis we use many of the basic results derived in the first part. We do not include results of numerical experiments with space-time TraceFEM. For this we refer to [23, 22].

The paper is organized as follows. In Sections 2 and 3 we collect basic facts of the level set function approximation $\phi_h \approx \phi$ and recall relevant properties of the parametric mapping that is used for the mesh deformation. We also explain how

functions defined on S or S_h are extended to a small neighborhood. In Section 4 we derive several useful integral transformation rules and a partial integration rule on S_h^n , which denotes the n th time slab part of S_h . We also show how for a function defined on S its space-time surface gradient can be expressed in terms of a space-time surface gradient on S_h of an extension of this function. In Section 5 bounds for certain geometric quantities, e.g., the change in surface measure between S and S_h or the jump in certain conormals on S_h are derived. In Section 6 we consider the standard model of a surfactant equation on a smoothly evolving surface and outline the space-time TraceFEM applied to this surface PDE. In Section 7 we present an error analysis of this method. This analysis has a standard structure, based on a space-time stability estimate, a Strang Lemma, consistency estimates and interpolation error bounds. The main result is given in Theorem 7.8, which contains optimal order error bounds for the space-time TraceFEM.

2. Level set representation of the continuous space-time surface. We introduce a space-time surface that is characterized using a level set function. For a domain $\Omega \subset \mathbb{R}^3$, $T > 0$, a smooth velocity field $\mathbf{w} : \Omega \times [0, T] \rightarrow \mathbb{R}^3$ and an initialization $\phi_0 : \Omega \rightarrow \mathbb{R}$, assume that the level set function $\phi : \Omega \times [0, T] \rightarrow \mathbb{R}$ solves the level set equation $\frac{\partial \phi}{\partial t} + \mathbf{w} \cdot \nabla \phi = 0$ and satisfies $\phi(\cdot, 0) = \phi_0$. Furthermore we assume that the zero level

$$\Gamma(t) = \{\mathbf{x} \in \Omega : \phi(\mathbf{x}, t) = 0\}$$

is a closed, connected and orientable C^2 -hypersurface for all $t \in [0, T]$. This in particular implies that the zero level $\Gamma(0)$ is advected by \mathbf{w} . The corresponding smooth space-time surface is denoted by

$$S := \bigcup_{t \in [0, T]} (\Gamma(t) \times \{t\}) \subset \mathbb{R}^4.$$

In the following, we use \lesssim and \gtrsim for inequalities that hold with constants independent of mesh size, time step size and cut configuration within the mesh. We use \sim to denote that both \lesssim and \gtrsim hold.

ASSUMPTION 2.1. *We assume the following standard properties of a level set function. For all (\mathbf{x}, t) in a neighborhood $U \subset \mathbb{R}^4$ of S :*

$$\|\nabla \phi(\mathbf{x}, t)\| \sim 1, \quad \|D^2 \phi(\mathbf{x}, t)\| \lesssim 1, \quad \|\partial_t \phi\| \lesssim 1, \quad \|\partial_t \nabla \phi\| \lesssim 1, \quad (2.1)$$

and for all $t \in [0, T]$, $\epsilon, \tilde{\epsilon} \in [0, \epsilon_0]$, $\epsilon_0 > 0$ sufficiently small:

$$|\phi(\mathbf{x} + \epsilon \nabla \phi(\mathbf{x}), t) - \phi(\mathbf{x} + \tilde{\epsilon} \nabla \phi(\mathbf{x}), t)| \sim |\epsilon - \tilde{\epsilon}|, \quad \mathbf{x} \in U(t), \quad (2.2)$$

where $U(t) \subset \Omega$ is such that $U = \bigcup_{t \in [0, T]} U(t) \times \{t\}$.

The spatial unit outer normal $\mathbf{n} : S \rightarrow \mathbb{R}^3$ and the space-time unit outer normal $\mathbf{n}_S : S \rightarrow \mathbb{R}^4$ are given by

$$\mathbf{n} := \frac{\nabla \phi}{\|\nabla \phi\|} \quad \text{and} \quad \mathbf{n}_S := \frac{\nabla_{(\mathbf{x}, t)} \phi}{\|\nabla_{(\mathbf{x}, t)} \phi\|}. \quad (2.3)$$

On S the following relation between \mathbf{n} and \mathbf{n}_S holds:

$$\mathbf{n}_S = \frac{1}{\alpha} \begin{pmatrix} \mathbf{n} \\ -V \end{pmatrix}, \quad V := \mathbf{w} \cdot \mathbf{n}, \quad \alpha := \sqrt{1 + V^2}. \quad (2.4)$$

Note that $V = \mathbf{w} \cdot \mathbf{n}$ is the normal velocity of the evolving surface $\Gamma(t)$ and satisfies

$$V = \frac{-1}{\|\nabla\phi\|} \frac{\partial\phi}{\partial t}. \quad (2.5)$$

Let ds and $d\sigma$ be the surface measures on $\Gamma(t)$ and S respectively. The integral transformation formula

$$\int_0^T \int_{\Gamma(t)} g \, ds \, dt = \int_S \frac{g}{\alpha} \, d\sigma, \quad g \in L^2(S), \quad (2.6)$$

holds, cf. [22, Appendix A.1] for a proof. Clearly we could also use the transformation formula (2.6) in a different form, with αg and g on the left-hand side and right-hand side, respectively. We use the form (2.6) because in the application in Section 6 we use tensor product spaces, which fit naturally to the space-time integral (without any scaling) as in the left-hand side of (2.6). One important result in Section 4 (Corollary 4.5) is an analogue of (2.6) for a space-time surface approximation that has only Lipschitz smoothness.

3. Approximation of the space-time surface. In the context of discretization of surface partial differential equations on evolving surfaces it is natural to use a time stepping procedure. For $N \in \mathbb{N}$, let the time interval $[0, T]$ be partitioned into smaller time intervals $I_n := [t_{n-1}, t_n]$, $1 \leq n \leq N$, where $0 = t_0 < t_1 < \dots < t_N = T$. We define $Q := \Omega \times [0, T] \subset \mathbb{R}^4$ and for $n = 1, \dots, N$, we define the space-time cylinders and corresponding space-time surface

$$Q_n := \Omega \times I_n, \quad S^n := \bigcup_{t \in I_n} (\Gamma(t) \times \{t\}).$$

Let \mathcal{T} be an element of a family $\{\mathcal{T}_h\}_{h>0}$ of shape regular tetrahedral triangulations of Ω , the triangulation $Q_{h,n} := \mathcal{T} \times I_n$ divides the time slab Q_n into space-time prismatic elements. The space-time triangulation of Q is denoted by $Q_h := \bigcup_{n=1}^N Q_{h,n}$. To simplify the presentation and the analysis we do not allow a change of triangulation between time slabs. Let V_h^m , $m \in \mathbb{N}$, be the standard $H^1(\Omega)$ -conforming finite element space of piecewise polynomials up to degree m on the triangulation \mathcal{T} . For $m_s, m_q \in \mathbb{N}$ a space-time finite element product space is given by

$$V_h^{m_s, m_q} := \{v : Q \rightarrow \mathbb{R} : v|_{Q_n}(\mathbf{x}, t) = \sum_{i=0}^{m_q} t^i v_i(\mathbf{x}), \quad v_i \in V_h^{m_s}, \quad 1 \leq n \leq N\}. \quad (3.1)$$

Note that functions from $V_h^{m_s, m_q}$ are continuous in space but may be discontinuous in time at the time interval boundaries t_n . This finite element space is used both in the finite element discretization of the surface PDE studied in Section 6 and, with possibly different degrees m_s, m_q , in the parametric mapping used for the higher order geometry approximation. For the geometry approximation we assume a $\phi_h \in V_h^{k_{g,s}, k_{g,q}}$, i.e., with degree $k_{g,s}$ in \mathbf{x} and $k_{g,q}$ in t . Such a ϕ_h may be an interpolation of ϕ , if the latter is available. In applications, ϕ may be determined implicitly by a level set equation. For a higher order surface approximation we need a sufficiently accurate approximation $\phi_h \approx \phi$. Requirements for the accuracy of ϕ_h as approximation of ϕ are specified below, cf. Assumption 5.1.

The evaluation of integrals on the zero level of a higher order polynomial (e.g., ϕ_h) requires (too) much computational effort. This motivates the use of an approach

that is similar to the classical parametric finite element method. Below we explain the basic structure of the space-time parametric technique introduced and analyzed in [12, 11]. For further details we refer to this literature and to [21, 22, 23].

REMARK 3.1. In [12, 11] two different techniques for construction of the space-time parametric mapping are presented, one based on the *FE blending* and the other one based on a *smooth blending*. For the purpose of space-time discretization of surface PDEs the technique based on FE blending is the most natural (and simpler) choice, cf. [11, Remark 3.1]. In the present paper we therefore restrict to the construction of Θ_h^n based on FE blending.

By \mathcal{I}_m we denote the spatial nodal interpolation operator in V_h^m . The spatially piecewise linear nodal interpolation is denoted by $\hat{\phi}_h \in V_h^{1,k_{g,q}}$:

$$\hat{\phi}_h(\cdot, t) := \mathcal{I}_1 \phi_h(\cdot, t) \in V_h^1, \quad t \in [0, T], \quad (3.2)$$

and its corresponding piecewise planar zero level at time t

$$\Gamma_{\text{lin}}(t) := \left\{ \mathbf{x} \in \Omega : \hat{\phi}_h(\mathbf{x}, t) = 0 \right\},$$

which is easy to compute. This surface $\Gamma_{\text{lin}}(t)$ is a (only) second order accurate approximation of $\Gamma(t)$. The corresponding discrete space-time surface is denoted by

$$S_{\text{lin}}^n := \left\{ (\mathbf{x}, t) \in Q_n : \hat{\phi}_h(\mathbf{x}, t) = 0 \right\}, \quad S_{\text{lin}} := \bigcup_{n=1}^N S_{\text{lin}}^n.$$

We consider all elements that are cut by the piecewise linear surface at a point in time within one time slab and the corresponding space-time prisms, i.e.,

$$\begin{aligned} \mathcal{T}_n^\Gamma &:= \{ K \in \mathcal{T} : \text{meas}_2((K \times I_n) \cap \Gamma_{\text{lin}}(t)) > 0 \text{ for a } t \in I_n \}, \\ Q_{h,n}^S &:= \mathcal{T}_n^\Gamma \times I_n, \quad n \in \{1, \dots, N\}, \end{aligned}$$

and $Q_h^S := \cup_{n=1}^N Q_{h,n}^S$. The corresponding domains are denoted by $\Omega_n^\Gamma := \{ \mathbf{x} \in K : K \in \mathcal{T}_n^\Gamma \}$, $Q_n^S = \Omega_n^\Gamma \times I_n$ and $Q^S = \cup_{n=1}^N Q_n^S$. In the remainder we assume $Q^S \subset U$ (which is satisfied for h and Δt sufficiently small).

The construction of the mesh deformation is based on an “ideal” spatial mapping $\Psi_t : U(t) \rightarrow \mathbb{R}^3$ that depends on the level set function ϕ and for which $\Psi_t(\Gamma_{\text{lin}}(t)) = \Gamma(t)$ holds. A corresponding space-time mapping is given by $\Psi : U \rightarrow \mathbb{R}^4$, $\Psi(\mathbf{x}, t) := (\Psi_t(\mathbf{x}), t)$. This mapping Ψ is continuous on U . By $\mathcal{P}^{k_{g,q}}(I_n)$ we denote the space of polynomials up to degree $k_{g,q}$ on I_n . Let $\tau_m^n \in I_n$, $m = 0, \dots, k_{g,q}$, be discrete points and $\mathcal{X}_{\tau_m^n} \in \mathcal{P}^{k_{g,q}}(I_n)$ corresponding finite element nodal basis functions. On I_n the function Ψ_t is interpolated in t by $\tilde{\Psi}_t(\mathbf{x}) = \sum_{m=0}^{k_{g,q}} \mathcal{X}_{\tau_m^n}(t) \Psi_{\tau_m^n}(\mathbf{x})$. For given $t = \tau_m^n$ a mapping $\Theta_{h,t}^n \approx \Psi_t$ is constructed. This mapping, which deforms all elements of the triangulation \mathcal{T}_n^Γ and depends (only) on ϕ_h , is such that $\Theta_{h,t}^n \in (V_h^{k_{g,s}})^3$. The spatial mesh deformation $\Theta_{h,s}^n \in (V_h^{k_{g,s}, k_{g,q}})^3$ and the corresponding space-time mapping Θ_h^n are defined by

$$\Theta_{h,s}^n(\mathbf{x}, t) := \sum_{m=0}^{k_{g,q}} \mathcal{X}_{\tau_m^n}(t) \Theta_{h,\tau_m^n}^n(\mathbf{x}), \quad \Theta_h^n(\mathbf{x}, t) := (\Theta_{h,s}^n(\mathbf{x}, t), t), \quad (\mathbf{x}, t) \in Q_n^S, \quad (3.3)$$

cf. Fig. 3.1 for an illustration.

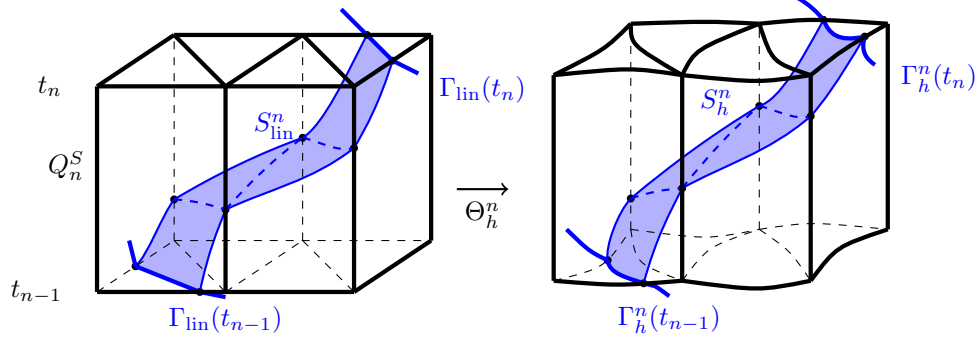


Fig. 3.1: The mapping Θ_h^n , defined on $Q_{h,n}^S$, deforms the surface S_{lin} . Note that S_{lin} is piecewise linear in space only.

We note that opposite to the ideal mapping Ψ , the mesh deformation Θ_h^n is *not* necessarily continuous between time slabs, cf. Remark 3.2. Using this mesh deformation we obtain the *space-time surface approximation*

$$S_h^n := \{(\mathbf{x}, t) \in Q_n : (\mathbf{x}, t) \in \Theta_h^n(S_{\text{lin}}^n)\}, \quad 1 \leq n \leq N, \quad S_h := \bigcup_{n=1}^N S_h^n. \quad (3.4)$$

The accuracy of the approximation $S_h \approx S$ is discussed in Section 5. The corresponding time slices of S_h^n are denoted by

$$\Gamma_h^n(t) := \{\mathbf{x} \in \mathbb{R}^3 : (\mathbf{x}, t) \in S_h^n\}, \quad t \in I_n, \quad n = 1, \dots, N. \quad (3.5)$$

For a given n and almost everywhere on Q_n^S we define (with $D\Theta$ the spatial Jacobian of Θ)

$$\mathbf{n}_{\text{lin}} := \frac{\nabla \hat{\phi}_h}{\|\nabla \hat{\phi}_h\|}, \quad \mathbf{n}_h \circ \Theta_h^n := \frac{(D\Theta_{h,s}^n)^{-T} \mathbf{n}_{\text{lin}}}{\|(D\Theta_{h,s}^n)^{-T} \mathbf{n}_{\text{lin}}\|}, \quad (3.6)$$

with $\hat{\phi}_h$ as defined in (3.2) and $\Theta_{h,s}^n$ as in (3.3). Restricted to $\Gamma_{\text{lin}}(t)$ these vectors are indeed the unit (spatial) normal vectors to the surface approximations $\Gamma_{\text{lin}}(t)$ and $\Gamma_h^n(t)$, respectively. On Q_n^S we also introduce space-time variants:

$$\mathbf{n}_{S_{\text{lin}}} := \frac{\nabla_{(\mathbf{x},t)} \hat{\phi}_h}{\|\nabla_{(\mathbf{x},t)} \hat{\phi}_h\|}, \quad \mathbf{n}_{S_h} \circ \Theta_h^n := \frac{(D_{(\mathbf{x},t)} \Theta_h^n)^{-T} \mathbf{n}_{S_{\text{lin}}}}{\|(D_{(\mathbf{x},t)} \Theta_h^n)^{-T} \mathbf{n}_{S_{\text{lin}}}\|}. \quad (3.7)$$

On S_{lin}^n these normals are the unit space-time normals to the respective space-time surfaces, cf. [22, Subsection 4.2.4] for more discussion.

We introduce a discrete variant of the normal velocity $V = \mathbf{w} \cdot \mathbf{n}$, cf. (2.5). Almost everywhere on S_h^n , $n = 1, \dots, N$, we define

$$V_h := \frac{-\frac{\partial(\hat{\phi}_h \circ (\Theta_h^n)^{-1})}{\partial t}}{\|\nabla(\hat{\phi}_h \circ (\Theta_h^n)^{-1})\|} = \frac{-\left(\frac{\partial(\Theta_h^n)^{-1}}{\partial t}\right)^T \left(\nabla_{(\mathbf{x},t)} \hat{\phi}_h \circ (\Theta_h^n)^{-1}\right)}{\|(D\Theta_{h,s}^n)^{-T} \nabla \hat{\phi}_h\| \circ (\Theta_h^n)^{-1}}. \quad (3.8)$$

We will use this V_h in Section 4. Its analogue on S_{lin} reads

$$V_{\text{lin}} := \frac{-1}{\|\nabla \hat{\phi}_h\|} \frac{\partial \hat{\phi}_h}{\partial t}. \quad (3.9)$$

REMARK 3.2. The construction of Θ_h^n based on FE blending, cf. Remark 3.1, leads to surface discontinuities between time slabs (which is not the case for the smooth blending approach). We briefly explain the origin of these discontinuities, cf. [11, Remark 5.3]. Take a fixed $t = t_n$ and let $K \in \mathcal{T}$ be a tetrahedron that is cut by $\Gamma_{\text{lin}}(t_n)$. By construction we then have $K \in \mathcal{T}_n^\Gamma \cap \mathcal{T}_{n+1}^\Gamma$. The sets of neighboring tetrahedra of K in \mathcal{T}_n^Γ and in \mathcal{T}_{n+1}^Γ , however, are not necessarily the same. Due to an averaging at the finite element nodes used in the construction of $\Theta_{h,t}^n$, cf. [16, 7, 11], the mappings Θ_{h,t_n}^n and Θ_{h,t_n}^{n+1} are in general not the same on K . Thus, for certain $\mathbf{x} \in \Omega_n^\Gamma \cap \Omega_{n+1}^\Gamma$ we have

$$\Theta_{h,s}^{n+1}(\mathbf{x}, t_n) = \Theta_{h,t_n}^{n+1}(\mathbf{x}) \neq \Theta_{h,t_n}^n(\mathbf{x}) = \Theta_{h,s}^n(\mathbf{x}, t_n),$$

which in particular implies $\Gamma_h^{n+1}(t_n) \neq \Gamma^n(t_n)$. In a discretization method the transfer of information between time slabs has to take this possible surface discontinuity into account, cf. Section 6.1.

3.1. Extension techniques. We briefly recall a standard closest point projection that we use to extend functions, that are defined only on S or S_h , to a neighborhood. We extend \mathbf{n} , cf. 2.3, spatially in a canonical way through the spatial signed distance function. We use the same *spatial-only* extension for the *space-time* normal \mathbf{n}_S . Let U be a sufficiently small neighborhood of S such that the spatial signed distance function to $\Gamma(t)$, denoted by $\delta(\cdot, t) : U(t) \rightarrow \mathbb{R}$ is C^1 . The extension of \mathbf{n} is given by $\mathbf{n}(\mathbf{x}, t) := \nabla \delta(\mathbf{x}, t)$, $(\mathbf{x}, t) \in U$. The (spatial) closest point projection is defined as

$$\mathbf{p} : U \rightarrow S, \quad \mathbf{p}(\mathbf{x}, t) := (\mathbf{x} - \delta(\mathbf{x}, t)\mathbf{n}(\mathbf{x}, t), t). \quad (3.10)$$

This induces the unique decomposition

$$(\mathbf{x}, t) = \mathbf{p}(\mathbf{x}, t) + \delta(\mathbf{x}, t)(\mathbf{n}(\mathbf{x}, t), 0), \quad (\mathbf{x}, t) \in U.$$

It follows that the restriction $\mathbf{p}|_{S_h^n} : S_h^n \rightarrow S^n$, $n = 1, \dots, N$, is bijective. For $n = 1, \dots, N$, we define $\mathbf{p}_n^{-1} : S^n \rightarrow S_h^n$, $\mathbf{p}_n^{-1}(\mathbf{x}, t) := (\mathbf{p}|_{S_h^n})^{-1}(\mathbf{x}, t)$. For a function $v : S \rightarrow \mathbb{R}$ we define its extension $v^e : U \rightarrow \mathbb{R}$ by

$$v^e(\mathbf{x}, t) := v(\mathbf{p}(\mathbf{x}, t)). \quad (3.11)$$

Similarly, for a function $v_h : S_h^n \rightarrow \mathbb{R}$ we define its extension $v_h^l : U^n := U|_{\mathbb{R}^3 \times I_n} \rightarrow \mathbb{R}$ by

$$v_h^l(\mathbf{x}, t) := \begin{cases} v_h(\mathbf{p}_n^{-1}(\mathbf{x}, t)), & (\mathbf{x}, t) \in S^n \\ v_h^l(\mathbf{p}(\mathbf{x}, t)), & (\mathbf{x}, t) \in U^n \setminus S^n \end{cases}. \quad (3.12)$$

Both extensions of functions on S and on S_h^n are constant extensions in the direction of \mathbf{n} . Also note that for the extended normal $\mathbf{n} = \nabla \delta$ we have $\mathbf{n} = \mathbf{n}^e$.

REMARK 3.3. In the analysis below we use extensions as in (3.11) and (3.12) that are based on the *spatial* closest point projection (3.10). In our space-time setting it may seem (more) natural to use a space-time closest point projection, i.e., $\mathbf{p}_S : U \rightarrow S$ with $\mathbf{p}_S(\mathbf{x}, t) := \operatorname{argmin}_{\mathbf{z} \in S} \|\mathbf{x}, t) - \mathbf{z}\|$. An important difference to the case with the closed smooth surface $\Gamma(t)$ above is that the space-time surface S and the time slab surfaces S^n have boundaries. It is easy to see that due to this, in general the mappings $\mathbf{p}_S|_{S_h^1}$ and $\mathbf{p}_S|_{S_h^N}$ (i.e. close to ∂S) are not injective. Also in general we have $\operatorname{Range}(\mathbf{p}_S|_{S_h^n}) \neq S^n$. In our analysis it is important (and natural) to use a bijection between S^n and S_h^n and time slab wise extensions. The space-time closest point projection is clearly not very suitable for constructing such a bijection and extensions. For these reasons we use the construction based on the spatial closest point projection.

4. Basic properties of the space-time surface approximation. In order to analyze discretization errors of finite element methods that use the surface approximation S_h one needs information about how certain surface characteristics on S relate to corresponding ones on S_h . In this section we present such results. We derive a formula that relates the space-time surface measure on S to that on S_h . We give a formula for the space-time normal on S_h that can be directly compared to the formula (2.4) for the space-time normal on S . Furthermore we present an analogue of the integral transformation formula (2.6) for the space-time surface approximation S_h and give a partial integration formula on the space-time surface approximation.

We start with a comparison of surface measures on S and S_h . Formulas that relate surface measures on $\Gamma(t)$ and $\Gamma_h(t)$ are known in the literature. We recall a result derived in [2, Proposition 2.5]. For any $t \in I_n$ let the two-dimensional surface measures of $\Gamma(t)$ and $\Gamma_h^n(t)$ be denoted by ds and ds_h , respectively. On $U(t)$ we define $\kappa_i := \frac{\kappa_i^e}{1 + \delta \kappa_i^e}$, where the principal curvatures κ_1, κ_2 and 0 are the three eigenvalues of the Weingarten mapping $\mathbf{H} := D\mathbf{n}$ on $U(t)$. On $\Gamma_h(t)$ let μ_h satisfy $\mu_h ds_h = ds \circ \mathbf{p}$. On $\Gamma_h(t)$ we then have

$$\mu_h = \mathbf{n} \cdot \mathbf{n}_h \prod_{i=1}^2 (1 - \delta \kappa_i). \quad (4.1)$$

The analysis in [2, Proposition 2.5], which also applies to d -dimensional hypersurfaces with $d \neq 2$, is *not* applicable to the space-time surface S and its approximation S_h . The reason for this is that in our setting we want to use (only) the space-distance function $\delta(\cdot, t)$ to $\Gamma(t)$ and not a space-time distance function to S . The result in the following lemma yields a useful result. A proof is given in the Appendix.

LEMMA 4.1. *Let the three-dimensional surface measures of S and S_h be denoted by $d\sigma$ and $d\sigma_h$, respectively. Let μ_h^S be such that $\mu_h^S d\sigma_h = d\sigma \circ \mathbf{p}$ on S_h^n . We define $\mathbf{n}_0^T := (\mathbf{n}^T, 0)$. For $1 \leq n \leq N$ we have, with α as in (2.4),*

$$\mu_h^S = \alpha^e \mathbf{n}_0 \cdot \mathbf{n}_{S_h} \prod_{i=1}^2 (1 - \delta \kappa_i) \quad \text{on } S_h^n. \quad (4.2)$$

Note that the result in (4.2) is general in the sense that it involves only geometric quantities related to S_h and S . The way S_h is constructed, e.g., in our case based on the space time mesh deformation Θ_h^n , does not play a role. Based on the formula for

μ_h^S in (4.2) we now derive a formula that relates the space-time surface integral to a product integral.

LEMMA 4.2. For $g \in L^2(S_h^n)$, $n = 1, \dots, N$, we have

$$\int_{t_{n-1}}^{t_n} \int_{\Gamma_h^n(t)} g \, ds_h \, dt = \int_{S_h^n} g \frac{\mathbf{n}_0 \cdot \mathbf{n}_{S_h}}{\mathbf{n} \cdot \mathbf{n}_h} \, d\sigma_h, \quad (4.3)$$

with $\mathbf{n}_0^T = (\mathbf{n}^T, 0)$.

Proof. We conclude using the continuous integral transformation (2.6) and the definitions of μ_h , μ_h^S given in (4.1) and (4.2)

$$\begin{aligned} \int_{t_{n-1}}^{t_n} \int_{\Gamma_h^n(t)} g \, ds_h \, dt &= \int_{t_{n-1}}^{t_n} \int_{\Gamma(t)} g^l \frac{1}{\mu_h^l} \, ds \, dt = \int_{S_h^n} g^l \frac{1}{\mu_h^l \alpha} \, d\sigma \\ &= \int_{S_h^n} g \frac{1}{\mu_h \alpha^e} \mu_h^S \, d\sigma_h = \int_{S_h^n} g \frac{\mathbf{n}_0 \cdot \mathbf{n}_{S_h}}{\mathbf{n} \cdot \mathbf{n}_h} \, d\sigma_h. \end{aligned} \quad (4.4)$$

□

The result (4.3) is not satisfactory, yet, because it involves the normal vector \mathbf{n} of the exact surface. Below, in Corollary 4.5, we derive a formula that is a direct discrete analogue of (2.6) and uses only quantities available in the discretization method. For this we need a discrete analogue of the relation (2.4), derived in Lemma 4.4 below. Note that (2.4) directly follows from (2.3) and the level set equation $\frac{\partial \phi}{\partial t} + \mathbf{w} \cdot \nabla \phi = 0$. We proceed analogously in the discrete setting. Due to the more complicated definitions of \mathbf{n}_h , \mathbf{n}_{S_h} and V_h the derivations are more technical. We start with auxiliary identities in the next lemma. The first two results (4.5)-(4.6) are simple discrete analogues of relations for the exact level set function. The third identity (4.7) is basically a transformation formula between the “linear” normal velocity V_{lin} and its higher order version V_h .

LEMMA 4.3. The following identities hold:

$$\mathbf{n}_{S_{\text{lin}}} = \frac{1}{\sqrt{1 + V_{\text{lin}}^2}} \begin{pmatrix} \mathbf{n}_{\text{lin}} \\ -V_{\text{lin}} \end{pmatrix} \quad \text{a.e. on } S_{\text{lin}} \quad (4.5)$$

$$\left\| \nabla_{(\mathbf{x}, t)} \hat{\phi}_h \right\| = \sqrt{1 + V_{\text{lin}}^2} \left\| \nabla \hat{\phi}_h \right\| \quad \text{a.e. on } S_{\text{lin}}, \quad (4.6)$$

$$\sqrt{1 + V_h^2} = \frac{\sqrt{1 + V_{\text{lin}}^2} \left\| (D_{(\mathbf{x}, t)} \Theta_h^n)^{-T} \mathbf{n}_{S_{\text{lin}}} \right\|}{\left\| (D \Theta_{h,s}^n)^{-T} \mathbf{n}_{\text{lin}} \right\|} \circ (\Theta_h^n)^{-1} \quad \text{a.e. on } S_h^n, \quad 1 \leq n \leq N. \quad (4.7)$$

Proof. From the definitions of \mathbf{n}_{lin} , $\mathbf{n}_{S_{\text{lin}}}$ and V_{lin} in (3.6), (3.7) and (3.9) we get (a.e. on S_{lin})

$$\mathbf{n}_{S_{\text{lin}}} = \frac{\nabla_{(\mathbf{x}, t)} \hat{\phi}_h}{\left\| \nabla_{(\mathbf{x}, t)} \hat{\phi}_h \right\|} = \frac{\nabla_{(\mathbf{x}, t)} \hat{\phi}_h}{\sqrt{1 + V_{\text{lin}}^2} \left\| \nabla \hat{\phi}_h \right\|} = \frac{1}{\sqrt{1 + V_{\text{lin}}^2}} \begin{pmatrix} \mathbf{n}_{\text{lin}} \\ -V_{\text{lin}} \end{pmatrix}.$$

From this the results (4.5) and (4.6) immediately follow. We now consider the identity (4.7). For the squared denominator in this relation we introduce the notation $g_{\Theta} := \left\| (D \Theta_{h,s}^n)^{-T} \mathbf{n}_{\text{lin}} \right\|^2 \circ (\Theta_h^n)^{-1}$. For the squared numerator we get, using the structure

of Θ_h^n (cf. (3.3)) and (4.5)

$$\begin{aligned}
& \left((1 + V_{\text{lin}}^2) \left\| (D_{(\mathbf{x},t)} \Theta_h^n)^{-T} \mathbf{n}_{S_{\text{lin}}} \right\|^2 \right) \circ (\Theta_h^n)^{-1} \\
&= (1 + V_{\text{lin}}^2 \circ (\Theta_h^n)^{-1}) \left\| D_{(\mathbf{x},t)}^T (\Theta_h^n)^{-1} \mathbf{n}_{S_{\text{lin}}} \circ (\Theta_h^n)^{-1} \right\|^2 \\
&= (1 + V_{\text{lin}}^2 \circ (\Theta_h^n)^{-1}) \left\| D^T (\Theta_{h,s}^n)^{-1} \left(\frac{\mathbf{n}_{\text{lin}}}{\sqrt{1 + V_{\text{lin}}^2}} \circ (\Theta_h^n)^{-1} \right) \right\|^2 \\
&\quad + (1 + V_{\text{lin}}^2 \circ (\Theta_h^n)^{-1}) \left\| \left(\frac{\partial (\Theta_h^n)^{-1}}{\partial t} \right)^T \left(\mathbf{n}_{S_{\text{lin}}} \circ (\Theta_h^n)^{-1} \right) \right\|^2 \\
&= g_\Theta + \left\| \left(\frac{\partial (\Theta_h^n)^{-1}}{\partial t} \right)^T \left(\frac{\nabla_{(\mathbf{x},t)} \hat{\phi}_h}{\|\nabla \hat{\phi}_h\|} \circ (\Theta_h^n)^{-1} \right) \right\|^2,
\end{aligned} \tag{4.8}$$

where in the last equality we used the relation $\sqrt{1 + V_{\text{lin}}^2} \|\nabla \hat{\phi}_h\| \mathbf{n}_{S_{\text{lin}}} = \nabla_{(\mathbf{x},t)} \hat{\phi}_h$. Hence, using $\|\hat{\phi}_h\| \mathbf{n}_{\text{lin}} = \nabla \hat{\phi}_h$ we conclude that it remains to verify the identity

$$\frac{\left\| \left(\frac{\partial (\Theta_h^n)^{-1}}{\partial t} \right)^T \left(\nabla_{(\mathbf{x},t)} \hat{\phi}_h \circ (\Theta_h^n)^{-1} \right) \right\|}{\left\| (D \Theta_{h,s}^n)^{-T} \nabla \hat{\phi}_h \right\| \circ (\Theta_h^n)^{-1}} = |V_h| := \frac{\left| \frac{\partial (\hat{\phi}_h \circ (\Theta_h^n)^{-1})}{\partial t} \right|}{\left\| \nabla \left(\hat{\phi}_h \circ (\Theta_h^n)^{-1} \right) \right\|}. \tag{4.9}$$

The numerators in (4.9) agree, which follows from the chain rule. The denominators also agree, which again follows from the chain rule and the fact that the spatial derivative of the last component of Θ_h^n vanishes, cf. (3.3). \square

We use Lemma 4.3 in the proof of the following lemma that relates the (higher order) discrete spatial normal \mathbf{n}_h and the (higher order) discrete space-time normal \mathbf{n}_{S_h} in a formula with the same structure as (2.4).

LEMMA 4.4. *Almost everywhere on S_h^n , $n = 1, \dots, N$, we have the identity*

$$\mathbf{n}_{S_h} = \frac{1}{\sqrt{1 + V_h^2}} \begin{pmatrix} \mathbf{n}_h \\ -V_h \end{pmatrix}. \tag{4.10}$$

Proof. Recall the formulas (3.6) and (3.8)

$$\mathbf{n}_h \circ \Theta_h^n = \frac{(D \Theta_{h,s}^n)^{-T} \mathbf{n}_{\text{lin}}}{\left\| (D \Theta_{h,s}^n)^{-T} \mathbf{n}_{\text{lin}} \right\|}, \quad V_h \circ \Theta_h^n = \frac{- \left(\frac{\partial (\Theta_h^n)^{-1}}{\partial t} \circ \Theta_h^n \right)^T \nabla_{(\mathbf{x},t)} \hat{\phi}_h}{\left\| (D \Theta_{h,s}^n)^{-T} \nabla \hat{\phi}_h \right\|}.$$

Using (3.7) and the structure of Θ_h^n , cf. (3.3) we obtain

$$\mathbf{n}_{S_h} \circ \Theta_h^n = \frac{1}{\left\| (D_{(\mathbf{x},t)} \Theta_h^n)^{-T} \mathbf{n}_{S_{\text{lin}}} \right\|} \begin{pmatrix} (D \Theta_{h,s}^n)^{-T} \left(\frac{\mathbf{n}_{\text{lin}}}{\sqrt{1 + V_{\text{lin}}^2}} \right) \\ \left(\frac{\partial (\Theta_h^n)^{-1}}{\partial t} \circ \Theta_h^n \right)^T \mathbf{n}_{S_{\text{lin}}} \end{pmatrix}. \tag{4.11}$$

From (4.7) we get

$$\left\| (D_{(\mathbf{x},t)} \Theta_h^n)^{-T} \mathbf{n}_{S_{\text{lin}}} \right\|^{-1} = \frac{\sqrt{1 + V_{\text{lin}}^2}}{\sqrt{1 + V_h^2 \circ \Theta_h^n}} \left\| (D \Theta_{h,s}^n)^{-T} \mathbf{n}_{\text{lin}} \right\|^{-1}.$$

Hence, for the first three components of the vector $\mathbf{n}_{S_h} \circ \Theta_h^n \in \mathbb{R}^4$ we get

$$\frac{(D\Theta_{h,s}^n)^{-T} \left(\frac{\mathbf{n}_{\text{lin}}}{\sqrt{1+V_{\text{lin}}^2}} \right)}{\left\| (D_{(\mathbf{x},t)}\Theta_h^n)^{-T} \mathbf{n}_{S_{\text{lin}}} \right\|} = \frac{1}{\sqrt{1+V_h^2 \circ \Theta_h^n}} \mathbf{n}_h \circ \Theta_h^n,$$

and for the last entry we get, using (3.7), (4.6) and $\left\| \nabla \hat{\phi}_h \right\| \mathbf{n}_{\text{lin}} = \nabla \hat{\phi}_h$,

$$\frac{\left(\frac{\partial(\Theta_h^n)^{-1}}{\partial t} \circ \Theta_h^n \right)^T \mathbf{n}_{S_{\text{lin}}}}{\left\| (D_{(\mathbf{x},t)}\Theta_h^n)^{-T} \mathbf{n}_{S_{\text{lin}}} \right\|} = \frac{\left(\frac{\partial(\Theta_h^n)^{-1}}{\partial t} \circ \Theta_h^n \right)^T \nabla_{(\mathbf{x},t)} \hat{\phi}_h}{\sqrt{1+V_h^2 \circ \Theta_h^n} \left\| \nabla \hat{\phi}_h \right\| \left\| (D\Theta_{h,s}^n)^{-T} \mathbf{n}_{\text{lin}} \right\|} = \frac{-V_h \circ \Theta_h^n}{\sqrt{1+V_h^2 \circ \Theta_h^n}},$$

which completes the proof. \square

As an easy consequence we obtain a discrete analogue of the integral transformation formula.

COROLLARY 4.5. *For $g_h \in L^2(S_h^n)$, $n = 1, \dots, N$, we have*

$$\int_{t_{n-1}}^{t_n} \int_{\Gamma_h^n(t)} g_h \, ds_h \, dt = \int_{S_h^n} \frac{g_h}{\sqrt{1+V_h^2}} \, d\sigma_h. \quad (4.12)$$

Proof. The result follows from Lemma 4.2, Lemma 4.4 and $\mathbf{n}_0 \cdot \mathbf{n}_{S_h} = (1 + V_h^2)^{-\frac{1}{2}} \mathbf{n} \cdot \mathbf{n}_h$. \square

REMARK 4.6. We briefly comment on the structure of the proof of (4.12). A proof of (2.6) can be given using local parametrizations of $\Gamma(t)$ and of S , which can be related using the normal velocity $V = \mathbf{w} \cdot \mathbf{n}$ that transports $\Gamma(t)$. This approach does not work for the discrete version (4.12), because we do not have a velocity field available that transports $\Gamma_h^n(t)$. Instead, in our proof we relate integrals $\int_{\Gamma_h^n(t)} \sim \int_{\Gamma(t)}$ and $\int_{S_h^n} \sim \int_{S^n}$, and use the result (2.6).

Using Corollary 4.5 we are able to transform product integrals on $\Gamma_h^n(t) \times I_n$ to surface integrals on S_h^n . For the latter we have a natural partial integration formula, which is presented below in Theorem 4.7. A further useful relation between the surface measures on S and S_h , which follows from the results above, is given by

$$\frac{1}{\alpha} \, d\sigma = \frac{\mu_h}{\sqrt{1+V_h^2}} \, d\sigma_h. \quad (4.13)$$

4.1. Partial integration formula on the space-time surface approximation. Below we use standard surface differential operators on the smooth surfaces $\Gamma = \Gamma(t)$ (for fixed t) and S , denoted by ∇_γ (surface gradient) and div_γ , $\gamma \in \{\Gamma, S\}$. Corresponding to the velocity field \mathbf{w} we define the space-time vector $\mathbf{w}_S^T := (\mathbf{w}^T, 1) \in \mathbb{R}^4$. Elementary calculations, cf. [22, Lemma 3.2], yield the relation

$$\text{div}_S \left(\frac{1}{\alpha} \mathbf{w}_S \right) = \frac{1}{\alpha} \text{div}_\Gamma \mathbf{w} \quad \text{on } S. \quad (4.14)$$

For a scalar function $v \in H^1(S)$ the material derivative is given by

$$\dot{v} := \mathbf{w}_S \cdot \nabla_S v = \frac{\partial v^e}{\partial t} + \mathbf{w} \cdot \nabla v^e. \quad (4.15)$$

In our setting we are interested in partial integration for product integrals of the form $\int_0^T \int_{\Gamma(t)} g \, ds \, dt = \int_S \frac{1}{\alpha} g \, d\sigma$, with $\alpha = \sqrt{1 + (\mathbf{w} \cdot \mathbf{n})^2}$. The following partial integration formula holds

$$\begin{aligned} \int_S \frac{1}{\alpha} \dot{u} v \, d\sigma &= - \int_S \frac{1}{\alpha} u \dot{v} \, d\sigma + \int_S uv \operatorname{div}_S \left(\frac{1}{\alpha} \mathbf{w}_S \right) \, d\sigma \\ &+ \int_{\Gamma(T)} uv \, ds - \int_{\Gamma(0)} uv \, ds. \end{aligned} \quad (4.16)$$

This result can be derived using the Leibniz formula and the relation (4.14). In the setting of a finite element discretization on the space-time surface approximation S_h we are interested in a discrete analogue of (4.16).

Note that the space-time surface S_h^n is a Lipschitz surface formed by a triangulation of smooth curved space-time surfaces, cf. Figure 3.1 for the case of an evolving curve embedded in \mathbb{R}^2 . Let the space-time surface triangulation $\mathcal{T}_{S_h^n}$ be the set of smooth three-dimensional manifolds that S_h^n consists of, i.e.

$$\mathcal{T}_{S_h^n} := \{\Theta_h^n(P) \cap S_h^n : P \in Q_{h,n}^S\}.$$

Then, we have $S_h^n = \bigcup_{K_S \in \mathcal{T}_{S_h^n}} K_S$. Let $\mathcal{T}_{S_h} := \bigcup_{n=1}^N \mathcal{T}_{S_h^n}$. Note that $K_S \in \mathcal{T}_{S_h}$ is a three-dimensional curved polytope that can be partitioned into curved tetrahedra. In general this deformed triangulation \mathcal{T}_{S_h} is *not* shape regular; due to the evolving surface through the fixed bulk triangulation Q_h , element angles can be very small and the size of neighboring elements may vary strongly. An illustration of the two-dimensional analogue of $\mathcal{T}_{S_h^n}$ is given in Figure 3.1. For $n = 1, \dots, N$, let $\mathcal{F}_I^n := \{\partial K_S^1 \cap \partial K_S^2 : K_S^1, K_S^2 \in \mathcal{T}_{S_h^n}, K_S^1 \neq K_S^2\}$ be the set of interior curved boundary faces of the elements in $\mathcal{T}_{S_h^n}$ and let $\mathcal{F}_I := \bigcup_{n=1}^N \mathcal{F}_I^n$. Almost everywhere on ∂S_h^n the vector

$$\boldsymbol{\nu}_\partial := \frac{1}{\sqrt{1 + V_h^2}} \begin{pmatrix} V_h \mathbf{n}_h \\ 1 \end{pmatrix} \quad (4.17)$$

is orthogonal to ∂S_h^n and satisfies $\boldsymbol{\nu}_\partial \cdot \mathbf{n}_{S_h} = 0$, cf. (4.10). Hence, $\boldsymbol{\nu}_\partial$ is the unit conormal of the top boundary of S_h^n and $-\boldsymbol{\nu}_\partial$ is the unit outer conormal of the bottom boundary of S_h^n . For $K_S \in \mathcal{T}_{S_h}$ the interior conormals are denoted by $\boldsymbol{\nu}_h|_{K_S}$, cf. Figure 4.1 for an illustration.

Let $F \in \mathcal{F}_I^n$ be an interior curved boundary face with $F = K_S^1 \cap K_S^2$, $K_S^1, K_S^2 \in \mathcal{T}_{S_h^n}$. For a function v defined on $K_S^1 \cup K_S^2$ we define the (vector valued) conormal jump on F :

$$[v]_{\boldsymbol{\nu}}|_F := (v|_{K_S^1} \boldsymbol{\nu}_h|_{K_S^1} + v|_{K_S^2} \boldsymbol{\nu}_h|_{K_S^2})|_F. \quad (4.18)$$

Note that in general for the Lipschitz surface S_h^n we do not have C^1 smoothness across F and thus $\boldsymbol{\nu}_h|_{K_S^1} \neq -\boldsymbol{\nu}_h|_{K_S^2}$ on F . If the function v is continuous across F we have $[v]_{\boldsymbol{\nu}}|_F = v|_F [1]_{\boldsymbol{\nu}}|_F$. For one-sided values at the boundary of a time slab we use the standard notation

$$\begin{aligned} u_+^n &:= u_+(\cdot, t_n) = \lim_{\eta \searrow 0} u(\cdot, t_n + \eta), \quad n = 0, \dots, N-1, \\ u_-^n &:= u_-(\cdot, t_n) = \lim_{\eta \searrow 0} u(\cdot, t_n - \eta), \quad n = 1, \dots, N \end{aligned}$$

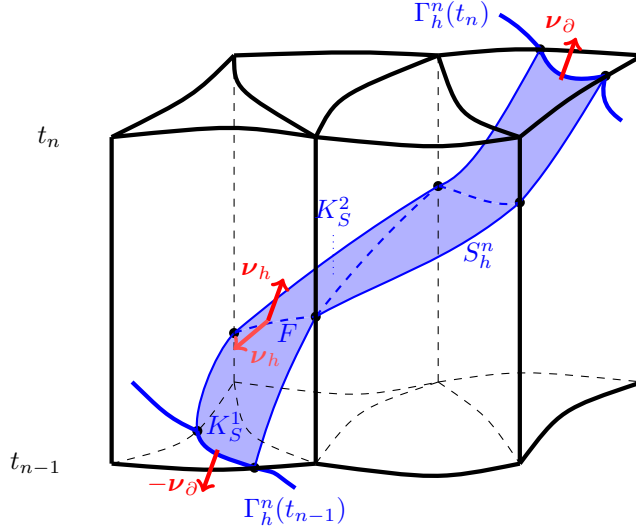


Fig. 4.1: The conormals $\pm \boldsymbol{\nu}_\partial$ at the time slab boundaries and the interior conormals $\boldsymbol{\nu}_h|_{K_S}$. Due to the non-smoothness of S_h , in general at a common face F one has $(\boldsymbol{\nu}_h|_{K_S^1})|_F \neq -(\boldsymbol{\nu}_h|_{K_S^2})|_F$.

and $u_-^0 := 0$. Besides a possible discontinuity in the (finite element) functions between time slabs we also can have a discontinuity in the space-time surface approximation S_h between S_h^n and S_h^{n+1} , cf. Remark 3.2. In view of this we introduce, for u defined on $S_h^n \cup S_h^{n+1}$ the jump

$$[u]_h^n := u_+^n - u_-^n \circ \Theta_h^n \circ (\Theta_h^{n+1})^{-1} \quad \text{on } \Gamma_h^{n+1}(t_n). \quad (4.19)$$

For $v \in H^1(S_h^n)$ we define the discrete material derivative as

$$\dot{v} := \mathbf{w}_S \cdot \nabla_{S_h} v = (\mathbf{P}_{S_h} \mathbf{w}_S) \cdot \nabla_{S_h} v, \quad \mathbf{P}_{S_h} := \mathbf{I} - \mathbf{n}_{S_h} \mathbf{n}_{S_h}^T. \quad (4.20)$$

This derivative is a.e. tangential to the space-time surface approximation S_h . In the next theorem we give a discrete analogue of the partial integration formula (4.16). A proof of this result can be found in [23, Appendix A].

THEOREM 4.7. *On S_h^n , $n = 1, \dots, N$, we consider a strictly positive piecewise smooth function $\alpha_h \in \bigoplus_{K_S \in \mathcal{T}_{S_h^n}} C^1(K_S)$ and $R := \alpha_h^{-1} \mathbf{w}_S \cdot \boldsymbol{\nu}_\partial$. For $u, v \in H^1(S_h^n)$, the following identity holds:*

$$\begin{aligned} \int_{S_h^n} \frac{1}{\alpha_h} \dot{u} v \, d\sigma_h &= - \int_{S_h^n} \frac{1}{\alpha_h} u \dot{v} \, d\sigma_h + \int_{\Gamma_h^n(t_n)} u_-^n v_-^n R_-^n \, d\sigma_h \\ &\quad - \int_{\Gamma_h^n(t_{n-1})} u_+^{n-1} v_+^{n-1} R_+^{n-1} \, d\sigma_h + \sum_{F \in \mathcal{F}_I^n} \int_F u v \mathbf{w}_S \cdot [\alpha_h^{-1}]_\nu \, dF \\ &\quad - \sum_{K_S \in \mathcal{T}_{S_h^n}} \int_{K_S} u v \operatorname{div}_{S_h} \left(\frac{1}{\alpha_h} \mathbf{P}_{S_h} \mathbf{w}_S \right) \, d\sigma_h. \end{aligned} \quad (4.21)$$

We briefly comment on the result (4.21). Comparing this identity with its continuous analogue (4.16), we observe a similar structure. The general function α_h serves as a discrete variant of the term α . Due to the non-smoothness of S_h^n , the identity (4.21) reveals several perturbations which are not present in (4.16) but are natural. The identity (4.21) is equal to (4.16) if we neglect geometry errors and consider $\alpha_h = \alpha$, in particular we then have $S_h = S$, $R = 1$ and $[\alpha_h^{-1}]_\nu|_F = 0$. Similar conormal jump terms between elements as in (4.21) naturally occur in the DG framework as well.

4.2. Transformation between space-time surface differential operators.

In this section we derive useful transformation formulas between continuous and discrete space-time differential operators, similar to the stationary setting, as in e.g., [3, Section 2.3], where the identity

$$(\nabla_\Gamma v_h^l)^e = (\mathbf{I} - \delta\mathbf{H})^{-1} \tilde{\mathbf{P}}_h \nabla_{\Gamma_h} v, \quad v_h \in H^1(S_h^n), \quad (4.22)$$

with $\tilde{\mathbf{P}}_h := \mathbf{I} - \frac{\mathbf{n}_h \mathbf{n}_h^T}{\mathbf{n}_h \cdot \mathbf{n}}$ is shown. On S_h we define

$$\mathbf{A}_h := \frac{\mu_h}{\sqrt{1 + V_h^2}} \tilde{\mathbf{P}}_h (\mathbf{I} - \delta\mathbf{H})^{-2} \tilde{\mathbf{P}}_h. \quad (4.23)$$

As in [3, Section 2.3], we obtain from (4.1), Corollary 4.5 and (4.22) the relation

$$\int_{S^n} \frac{1}{\alpha} \nabla_\Gamma u_h^l \cdot \nabla_\Gamma v_h^l \, d\sigma = \int_{S_h^n} \mathbf{A}_h \nabla_{\Gamma_h} u_h \cdot \nabla_{\Gamma_h} v_h \, d\sigma_h, \quad u_h, v_h \in H^1(S_h^n). \quad (4.24)$$

We establish a similar relation as in (4.22) but now with space-time gradients. The result (4.22) can not directly be applied in our space-time setting, as the projection \mathbf{p} acts orthogonal to $\Gamma(t)$, but not to S . We introduce the following (4×4) -matrices defined on U :

$$\mathbf{P}_0 := \mathbf{I} - \frac{\mathbf{n}_{S_h} \mathbf{n}_0^T}{\mathbf{n}_{S_h} \cdot \mathbf{n}_0}, \quad \tilde{\mathbf{D}} := \begin{pmatrix} \mathbf{I} - \delta\mathbf{H} & -V^e \mathbf{n} \\ -\delta \frac{\partial \mathbf{n}}{\partial t} & (\alpha^e)^2 \end{pmatrix}, \quad (4.25)$$

where $\mathbf{n}_0^T = (\mathbf{n}^T, 0)$. Using $\mathbf{n} \cdot \frac{\partial \mathbf{n}}{\partial t} = 0$ it follows that $\det(\tilde{\mathbf{D}}) = (\alpha^e)^2 \det(\mathbf{I} - \delta\mathbf{H}) > 0$, hence $\tilde{\mathbf{D}}$ invertible.

LEMMA 4.8. *For $1 \leq n \leq N$, the following holds:*

$$(\nabla_S v_h^l)^e = \tilde{\mathbf{D}}^{-1} \mathbf{P}_0 \nabla_{S_h} v_h, \quad v_h \in H^1(S_h^n). \quad (4.26)$$

Proof. We have

$$D_{(\mathbf{x}, t)} \mathbf{P} = \begin{pmatrix} (\mathbf{I} - \mathbf{m} \mathbf{n}^T - \delta\mathbf{H}) & V^e \mathbf{n} - \delta \frac{\partial \mathbf{n}}{\partial t} \\ 0 & 1 \end{pmatrix} =: \mathbf{D}_\mathbf{p}.$$

For the spatially extended space-time normal vector $\mathbf{n}_S^e := \frac{1}{\alpha^e} \begin{pmatrix} \mathbf{n} \\ -V^e \end{pmatrix}$ we define

$$\mathbf{P}_S^e := \mathbf{I} - \mathbf{n}_S^e (\mathbf{n}_S^e)^T = \begin{pmatrix} \mathbf{I} - \frac{\mathbf{m} \mathbf{n}^T}{(\alpha^e)^2} & \frac{V^e \mathbf{n}}{(\alpha^e)^2} \\ \frac{V^e \mathbf{n}^T}{(\alpha^e)^2} & \frac{1}{(\alpha^e)^2} \end{pmatrix}.$$

We have the relation $\mathbf{D}_{\mathbf{p}}^T = \tilde{\mathbf{D}}\mathbf{P}_S^e$. For $v_h \in H^1(S_h^n)$, the chain rule yields

$$\nabla_{(\mathbf{x},t)} v_h^l = \nabla_{(\mathbf{x},t)}(v_h^l \circ \mathbf{p}) = \mathbf{D}_{\mathbf{p}}^T(\nabla_{(\mathbf{x},t)} v_h^l) \circ \mathbf{p}.$$

Hence,

$$(\nabla_S v_h^l) \circ \mathbf{p} = \tilde{\mathbf{D}}^{-1} \nabla_{(\mathbf{x},t)} v_h^l. \quad (4.27)$$

Using $\mathbf{D}_{\mathbf{p}} \mathbf{n}_0 = 0$ on S_h^n we get $\nabla_{(\mathbf{x},t)} v_h^l = \mathbf{P}_0 \nabla_{(\mathbf{x},t)} v_h^l$ and combining this with $\mathbf{P}_0 = \mathbf{P}_0 \mathbf{P}_{S_h}$ we get

$$(\nabla_S v_h^l) \circ \mathbf{p} = \tilde{\mathbf{D}}^{-1} \mathbf{P}_0 \nabla_{S_h} v_h \quad \text{on } S_h^n.$$

□

5. Basic geometric error estimates. Recall that the approximate space-time surface is based on the parametric mesh deformation mapping Θ_h^n , cf. 3.4. Properties of this mapping and the related “ideal” mapping Ψ , cf. Section 3, are derived in the recent work [11]. Using these properties, bounds for the distance between S and S_h and between normals on S and S_h can be derived. Below in Lemma 5.2 we collect a few main results from [11] that are useful in our analysis. Based on these results we derive further estimates for geometric quantities (Lemma 5.3 and 5.6) and for differences between derivatives of a function on S_h and the derivatives of the corresponding lifted version on S .

Clearly, for higher order approximation results one needs assumptions on the accuracy of $\phi_h \approx \phi$. The following assumptions are introduced in [11, Assumptions 2.4, 2.5, 2.6].

ASSUMPTION 5.1. *We assume an approximation $\phi_h \in V_h^{k_{g,s}, k_{g,q}}$ of ϕ that satisfies for all $1 \leq n \leq N$ and $(m_s, m_q) \in (\{0, \dots, k_{g,s} + 1\} \times \{0, 1\}) \cup (\{0\} \times \{0, \dots, k_{g,q} + 1\})$*

$$\|D^{m_s} \partial_t^{m_q}(\phi_h - \phi)\|_{L^\infty(\mathcal{T}_n^\Gamma \times I_n)} \lesssim h^{k_{g,s} + 1 - m_s} + \Delta t^{k_{g,q} + 1 - m_q}. \quad (5.1)$$

Represent ϕ_h as $\phi_h(\mathbf{x}, t) = \sum_{m=0}^{k_{g,q}} \mathcal{X}_{\tau_m^n}(t) \phi_{h, \tau_m^n}(\mathbf{x})$, $t \in I_n$, $\phi_{h, \tau_m^n}(\mathbf{x}) := \phi_h(\mathbf{x}, \tau_m^n)$. We assume that for all $1 \leq n \leq N$ there exists $\phi_{\Delta t}(\mathbf{x}, t) = \sum_{m=0}^{k_{g,q}} \mathcal{X}_{\tau_m^n}(t) \phi_{\tau_m^n}(\mathbf{x})$, with $\phi_{\tau_m^n} \in C(\Omega) \cap C^{k_{g,s} + 1}(\Omega_n^\Gamma)$ such that the following holds:

$$\|D^{m_s}(\phi_{h, \tau_m^n} - \phi_{\tau_m^n})\|_{L^\infty(\mathcal{T}_n^\Gamma)} \lesssim h^{k_{g,s} + 1 - m_s}, \quad 0 \leq m_s \leq k_{g,s} + 1. \quad (5.2)$$

We assume that for all $1 \leq n \leq N$ there is $\phi_H \in C^{k_{g,q} + 1}(I_n; V_h^{k_{g,s}})$ such that for $m_q = 0, \dots, k_{g,q} + 1$ and $m_s \in \{0, 1\}$:

$$\|\partial_t^{m_q}(\phi_H - \phi_h)\|_{L^\infty(\mathcal{T}_n^\Gamma \times I_n)} \lesssim \Delta t^{k_{g,q} + 1 - m_q} \quad (5.3)$$

$$\|D^{m_s} \partial_t^{m_q}(\phi_H - \phi_h)\|_{L^\infty(\mathcal{T}_n^\Gamma \times I_n)} \lesssim h^{k_{g,s} + 1 - m_s} + \Delta t^{k_{g,q} + 1 - m_q}. \quad (5.4)$$

Note that these assumptions are satisfied if ϕ is sufficiently smooth and $\phi_h = I^t I^s \phi$ is a tensor product space time nodal interpolation in the finite element space $V_h^{k_{g,s}, k_{g,q}}$. One can then take $\phi_{\Delta t} = I^t \phi$ and $\phi_H = I^s \phi$. In the remainder of this paper we assume that Assumption 5.1 holds. The following results are derived in [11].

LEMMA 5.2.

$$\|\Theta_h^n - \Psi\|_{L^\infty(\mathcal{T}_n^\Gamma \times I_n)} \lesssim h^{k_{g,s}+1} + \Delta t^{k_{g,q}+1}, \quad (5.5)$$

$$\|D\Theta_h^n - D\Psi\|_{L^\infty(\mathcal{T}_n^\Gamma \times I_n)} \lesssim h^{k_{g,s}} + \Delta t^{k_{g,q}+1}, \quad (5.6)$$

$$\|\Theta_h^n - \text{id}\|_{L^\infty(\mathcal{T}_n^\Gamma \times I_n)} \lesssim h^2 + \Delta t^{k_{g,q}+1}, \quad (5.7)$$

$$\|\delta\|_{L^\infty(S_h)} \lesssim h^{k_{g,s}+1} + \Delta t^{k_{g,q}+1}, \quad (5.8)$$

$$\|\mathbf{n} - \mathbf{n}_h\|_{L^\infty(S_h)} \lesssim h^{k_{g,s}} + \Delta t^{k_{g,q}}, \quad (5.9)$$

$$\|\mathbf{n}_S^e - \mathbf{n}_{S_h}\|_{L^\infty(S_h)} \lesssim h^{k_{g,s}} + \Delta t^{k_{g,q}}. \quad (5.10)$$

Proof. The results (5.5) and (5.6) are given in [11, Theorem 4.12] and the result (5.7) follows from [11, Corollary 4.2] combined with (5.5). From (5.5) and (2.2) one easily derives the result (5.8), cf. [18, Lemma 3.8]. The result (5.9) is obtained from (5.5) and (5.6) with straightforward arguments, cf. [8, Lemma 3.3]. Concerning (5.10) we note the following. In [11, Lemma 5.12] the estimate

$$\|\mathbf{n}_S \circ \Phi_h^{st} - \mathbf{n}_{S_h}\|_{L^\infty(S_h)} \lesssim h^{k_{g,s}} + \Delta t^{k_{g,q}} \quad (5.11)$$

is proved. We refer to [11] for the definition of Φ_h^{st} , which satisfies $\|\Phi_h^{st} - \text{id}\|_{L^\infty(S_h)} \lesssim h^{k_{g,s}+1} + \Delta t^{k_{g,q}+1}$ (cf. [11, Corollary 5.9]). Using this we obtain

$$\begin{aligned} \|\mathbf{n}_S^e - \mathbf{n}_{S_h}\|_{L^\infty(S_h)} &= \|\mathbf{n}_S \circ \mathbf{p} - \mathbf{n}_{S_h}\|_{L^\infty(S_h)} \\ &\leq \|\mathbf{n}_S \circ \mathbf{p} - \mathbf{n}_S \circ \Phi_h^{st}\|_{L^\infty(S_h)} + \|\mathbf{n}_S \circ \Phi_h^{st} - \mathbf{n}_{S_h}\|_{L^\infty(S_h)} \\ &\lesssim \|\mathbf{p} - \text{id}\|_{L^\infty(S_h)} + \|\Phi_h^{st} - \text{id}\|_{L^\infty(S_h)} + \|\mathbf{n}_S \circ \Phi_h^{st} - \mathbf{n}_{S_h}\|_{L^\infty(S_h)}. \end{aligned}$$

Using $\|\mathbf{p} - \text{id}\|_{L^\infty(S_h)} = \|\delta\|_{L^\infty(S_h)}$ and the estimate (5.11) we obtain the result (5.10). \square

Without the assumptions (5.3) and (5.4) an extra term $h^{k_{g,s}+1}/\Delta t$ occurs in the bound in (5.10), cf. [11, Remark 5.13].

In the following lemma we derive bounds for differences between spatial surface measures on S and S_h and between space-time surface measures on S and S_h , cf. Lemma 4.1.

LEMMA 5.3. *The following uniform estimates hold:*

$$\|1 - \mu_h\|_{L^\infty(S_h)} \lesssim h^{k_{g,s}+1} + \Delta t^{k_{g,q}+1}, \quad (5.12)$$

$$\left\|1 - \mu_h^S\right\|_{L^\infty(S_h)} \lesssim h^{k_{g,s}} + \Delta t^{k_{g,q}}. \quad (5.13)$$

Proof. Using the identity $\mathbf{n} \cdot \mathbf{n}_h = 1 - \frac{\|\mathbf{n} - \mathbf{n}_h\|^2}{2}$ on S_h , the result (4.1), the uniform boundedness of the mean curvatures κ_i and (5.8)-(5.9), we obtain the estimate (5.12):

$$\begin{aligned} \|1 - \mu_h\|_{L^\infty(S_h)} &= \left\|1 - \left(1 - \frac{\|\mathbf{n} - \mathbf{n}_h\|^2}{2}\right) \prod_{i=1}^2 (1 - \kappa_i \delta)\right\|_{L^\infty(S_h)} \\ &\lesssim \|\delta\|_{L^\infty(S_h)} + \|\mathbf{n} - \mathbf{n}_h\|_{L^\infty(S_h)}^2 \lesssim h^{k_{g,s}+1} + \Delta t^{k_{g,q}+1}. \end{aligned}$$

Using the identity (4.2), the result (2.4) and the space-time normal bound (5.10) we obtain

$$\begin{aligned}
\left\| 1 - \mu_h^S \right\|_{L^\infty(S_h)} &= \left\| 1 - \alpha^e \mathbf{n}_0 \cdot \mathbf{n}_{S_h} \prod_{i=1}^2 (1 - \delta\kappa_i) \right\|_{L^\infty(S_h)} \\
&\lesssim \left\| 1 - \alpha^e \mathbf{n}_0 \cdot \mathbf{n}_S^e \right\|_{L^\infty(S_h)} + h^{k_{g,s}} + \Delta t^{k_{g,q}} \\
&\lesssim \left\| 1 - \mathbf{n}_0 \cdot \begin{pmatrix} \mathbf{n} \\ -V^e \end{pmatrix} \right\|_{L^\infty(S_h)} + h^{k_{g,s}} + \Delta t^{k_{g,q}} \\
&\lesssim \left\| 1 - \mathbf{n} \cdot \mathbf{n} \right\|_{L^\infty(S_h)} + h^{k_{g,s}} + \Delta t^{k_{g,q}} \lesssim h^{k_{g,s}} + \Delta t^{k_{g,q}},
\end{aligned}$$

which proves the estimate (5.13). \square

REMARK 5.4. Note that there is a loss of one power of h and of Δt in the bound for the space-time surface measure difference in (5.13) compared to the bound for the space surface measure difference in (5.12). These bounds are sharp and the reason for the loss of these powers is the following. The function $\mu_h(\mathbf{x}, t) = \frac{ds(\mathbf{p}(\mathbf{x}, t))}{ds_h(\mathbf{x}, t)}$ is the quotient of the surface measures of the interfaces $\Gamma(t)$ and $\Gamma_h^n(t)$, $n = 1, \dots, N$. The correspondence of points on $\Gamma_h(t)$ with points on $\Gamma(t)$ is given by the *orthogonal* (spatially) closest point projection \mathbf{p} . The function $\mu_h^S(\mathbf{x}, t) = \frac{d\sigma(\mathbf{p}(\mathbf{x}, t))}{d\sigma_h(\mathbf{x}, t)}$ is the quotient of the surface measures of the surfaces S and S_h^n , $n = 1, \dots, N$. For the correspondence of points on S_h^n with points on S the same projection \mathbf{p} is used, which, however, is in general *not* an orthogonal projection on S . This loss of the orthogonality property causes the loss of one power of h and of Δt .

REMARK 5.5. Using (4.1), (4.2) and (4.10) we get

$$\frac{\mu_h^S}{\mu_h} = \sqrt{1 + (V^2)^e} \frac{\mathbf{n}_0 \cdot \mathbf{n}_{S_h}}{\mathbf{n} \cdot \mathbf{n}_h} = \frac{\sqrt{1 + (V^e)^2}}{\sqrt{1 + V_h^2}} \quad \text{on } S_h^n.$$

Using this and (5.12)-(5.13) we see that (for $h \lesssim \Delta t$) V_h is an approximation of V^e of order (only) $\mathcal{O}(h^{k_{g,s}} + \Delta t^{k_{g,q}})$. In the application in Section 6 we need a more accurate approximation of V^e .

A further geometric quantity relevant for the accuracy of the space-time surface approximation S_h is the conormal jump $[\cdot]_{\boldsymbol{\nu}|_F}$ across interior faces $F \in \mathcal{F}_I$. In the next lemma we derive bounds for this quantity.

LEMMA 5.6. *For any curved face $F \in \mathcal{F}_I$ we have*

$$\left\| [1]_{\boldsymbol{\nu}|_F} \right\|_{L^\infty(F)} \lesssim h^{k_{g,s}} + \Delta t^{k_{g,q}}, \quad (5.14)$$

$$\left\| \mathbf{P}_S^e [1]_{\boldsymbol{\nu}|_F} \right\|_{L^\infty(F)} \lesssim h^{2k_{g,s}} + \Delta t^{2k_{g,q}}. \quad (5.15)$$

The conormal jump $[1]_{\boldsymbol{\nu}}$ is defined in (4.18).

Proof. Take an arbitrary $F \in \mathcal{F}_I$ and a fixed $(\mathbf{x}, t) \in F$. Let $\mathbf{s}_1, \mathbf{s}_2$ be two orthonormal vectors that span the tangent plane \hat{F} of the face F at (\mathbf{x}, t) . We omit the argument (\mathbf{x}, t) in this proof. Let $K_S^1, K_S^2 \in \mathcal{T}_{S_h}$ be the elements of the triangulation of the space-time surface with the common face F . We define the space-time normals on K_S^1, K_S^2 by $\mathbf{n}_1 := \mathbf{n}_{S_h^1}$ and $\mathbf{n}_2 := \mathbf{n}_{S_h^2}$ respectively. The corresponding conormals for F are denoted by $\boldsymbol{\nu}_1$ and $\boldsymbol{\nu}_2$. Note that $\{\mathbf{n}_1, \boldsymbol{\nu}_1, \mathbf{s}_1, \mathbf{s}_2\}$ and $\{\mathbf{n}_2, \boldsymbol{\nu}_2, \mathbf{s}_1, \mathbf{s}_2\}$ form

orthonormal bases in \mathbb{R}^4 and $\hat{F}^\perp = \text{span}\{\mathbf{n}_1, \boldsymbol{\nu}_1\} = \text{span}\{\mathbf{n}_2, \boldsymbol{\nu}_2\}$. We define the orthogonal matrix

$$Q := (\mathbf{n}_1 \ \boldsymbol{\nu}_1 \ \mathbf{s}_1 \ \mathbf{s}_2) (\boldsymbol{\nu}_1 \ -\mathbf{n}_1 \ \mathbf{s}_1 \ \mathbf{s}_2)^T = \mathbf{n}_1 \boldsymbol{\nu}_1^T - \boldsymbol{\nu}_1 (\mathbf{n}_1)^T + \mathbf{s}_1 \mathbf{s}_1^T + \mathbf{s}_2 \mathbf{s}_2^T,$$

which is a rotation by $\frac{\pi}{2}$ in the two-dimensional plane \hat{F}^\perp . We have $Q\boldsymbol{\nu}_1 = \mathbf{n}_1$ and $\boldsymbol{\nu}_2 \cdot Q\boldsymbol{\nu}_2 = 0$. From the latter and $F^\perp = \text{span}\{\mathbf{n}_2, \boldsymbol{\nu}_2\}$ it follows that $Q\boldsymbol{\nu}_2 = \pm\mathbf{n}_2$. By construction the angle between \mathbf{n}_1 and \mathbf{n}_2 is the same as between $\boldsymbol{\nu}_1$ and $-\boldsymbol{\nu}_2$, cf. Figure 5.1. Hence, $\mathbf{n}_1 \cdot \mathbf{n}_2 = -\boldsymbol{\nu}_1 \cdot \boldsymbol{\nu}_2 = -(Q\boldsymbol{\nu}_1) \cdot (Q\boldsymbol{\nu}_2) = -\mathbf{n}_1 \cdot Q\boldsymbol{\nu}_2$. We conclude that $Q\boldsymbol{\nu}_2 = -\mathbf{n}_2$ holds.

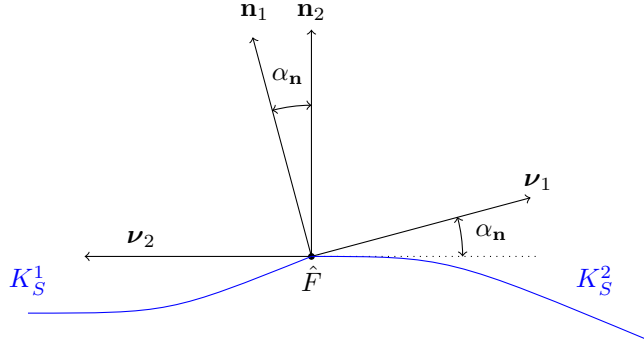


Fig. 5.1: Illustration of normals and conormals for two neighbouring elements $K_S^1, K_S^2 \in \mathcal{T}_{S_h}$.

Now let $\mathbf{n}_S^e = \mathbf{n}_S^e(\mathbf{x}, t)$ be the extended space-time normal to S , at $(\mathbf{x}, t) \in F$. Using (5.10) we get

$$\begin{aligned} \|[1]_\nu(\mathbf{x}, t)\| &= \|\boldsymbol{\nu}_1 + \boldsymbol{\nu}_2\| = \|Q(\boldsymbol{\nu}_1 + \boldsymbol{\nu}_2)\| = \|\mathbf{n}_1 - \mathbf{n}_2\| \\ &\lesssim \|\mathbf{n}_1 - \mathbf{n}_S^e\| + \|\mathbf{n}_S^e - \mathbf{n}_2\| \lesssim h^{k_{g,s}} + \Delta t^{k_{g,q}}, \end{aligned} \quad (5.16)$$

which yields (5.14). We turn to the proof of (5.15). We write $Q\mathbf{P}_S^e[1]_\nu = \alpha_1 \mathbf{n}_1 + \alpha_2 \boldsymbol{\nu}_1 + \beta_1 \mathbf{s}_1 + \beta_2 \mathbf{s}_2$. A straightforward computation yields

$$\begin{aligned} \alpha_1 &= 1 + \boldsymbol{\nu}_1 \cdot \boldsymbol{\nu}_2 - (\boldsymbol{\nu}_1 \cdot \mathbf{n}_S^e)^2 - \boldsymbol{\nu}_1 \cdot \mathbf{n}_S^e \mathbf{n}_S^e \cdot \boldsymbol{\nu}_2 \\ \alpha_2 &= -\mathbf{n}_1 \cdot \boldsymbol{\nu}_2 + \mathbf{n}_1 \cdot \mathbf{n}_S^e \mathbf{n}_S^e \cdot (\boldsymbol{\nu}_1 + \boldsymbol{\nu}_2) \\ \beta_i &= \mathbf{s}_i \cdot \mathbf{n}_S^e \mathbf{n}_S^e \cdot (\boldsymbol{\nu}_1 + \boldsymbol{\nu}_2), \quad i = 1, 2. \end{aligned}$$

Hence, $\|\mathbf{P}_S^e[1]_\nu\| = \|Q\mathbf{P}_S^e[1]_\nu\| = (\alpha_1^2 + \alpha_2^2 + \beta_1^2 + \beta_2^2)^{\frac{1}{2}}$. We introduce the notation $\epsilon := (1 + \frac{h}{\Delta t})h^{k_{g,s}} + \Delta t^{k_{g,q}}$ and use (cf. (5.16))

$$\begin{aligned} \|\boldsymbol{\nu}_1 + \boldsymbol{\nu}_2\| &\lesssim \epsilon, \quad |1 + \boldsymbol{\nu}_1 \cdot \boldsymbol{\nu}_2| = \frac{1}{2} \|\boldsymbol{\nu}_1 + \boldsymbol{\nu}_2\|^2 \lesssim \epsilon^2, \\ |\boldsymbol{\nu}_i \cdot \mathbf{n}_S^e| &= |\boldsymbol{\nu}_i \cdot (\mathbf{n}_S^e - \mathbf{n}_i)| \lesssim \epsilon, \quad i = 1, 2, \\ |\mathbf{s}_i \cdot \mathbf{n}_S^e| &= |\mathbf{s}_i \cdot (\mathbf{n}_S^e - \mathbf{n}_i)| \lesssim \epsilon, \quad i = 1, 2. \end{aligned}$$

Thus we get $|\alpha_1| \lesssim \epsilon^2$ and $|\beta_i| \lesssim \epsilon^2$, $i = 1, 2$. It remains to bound α_2 . Due to $\mathbf{n}_1 \cdot \mathbf{n}_S^e = 1 - \frac{1}{2} \|\mathbf{n}_1 - \mathbf{n}_S^e\|^2 = 1 + \mathcal{O}(\epsilon^2)$, cf. (5.10), and $\mathbf{n}_1 \cdot \boldsymbol{\nu}_1 = 0$ we obtain

$$|\alpha_2| \lesssim |(\mathbf{n}_S^e - \mathbf{n}_1) \cdot (\boldsymbol{\nu}_1 + \boldsymbol{\nu}_2)| \lesssim \epsilon^2.$$

Combining the results yields the estimate (5.15). \square

We now derive an estimate for the difference between a tangential gradient on S_h and the corresponding gradient on S of the lifted function. This useful result is an easy consequence of the relation given in Lemma 4.8.

LEMMA 5.7. *For all $v_h \in H^1(S_h^n)$ the following uniform estimate holds:*

$$\left\| \nabla_{S_h} v_h - (\nabla_S v_h^l)^e \right\|_{L^2(S_h^n)} \lesssim (h^{k_{g,s}} + \Delta t^{k_{g,q}}) \|\nabla_{S_h} v_h\|_{L^2(S_h^n)}. \quad (5.17)$$

Proof. From (4.26) we obtain, with \mathbf{P}_0 and $\tilde{\mathbf{D}}$ as in (4.25),

$$\nabla_{S_h} v_h - (\nabla_S v_h^l)^e = \nabla_{S_h} v_h - \tilde{\mathbf{D}}^{-1} \mathbf{P}_0 \nabla_{S_h} v_h = (\mathbf{P}_{S_h} - \tilde{\mathbf{D}}^{-1} \mathbf{P}_0) \nabla_{S_h} v_h. \quad (5.18)$$

From (4.26) it follows that $\tilde{\mathbf{D}}^{-1} \mathbf{P}_0 = \mathbf{P}_S^e \tilde{\mathbf{D}}^{-1} \mathbf{P}_0$ holds. The definition of $\tilde{\mathbf{D}}$ yields

$$\tilde{\mathbf{D}} = \mathbf{I} - \alpha^e V^e \begin{pmatrix} 0 & \mathbf{n}_S^e \\ \mathbf{n}_S^e & 0 \end{pmatrix} + \tilde{\mathbf{D}}_\Delta, \quad \tilde{\mathbf{D}}_\Delta := \begin{pmatrix} -\delta \mathbf{H} & 0 \\ -\delta \frac{\partial \mathbf{n}}{\partial t} & 0 \end{pmatrix},$$

and thus $\mathbf{P}_S^e \tilde{\mathbf{D}} = \mathbf{P}_S^e + \mathbf{P}_S^e \tilde{\mathbf{D}}_\Delta$, i.e., $\mathbf{P}_S^e \tilde{\mathbf{D}}^{-1} = \mathbf{P}_S^e - \mathbf{P}_S^e \tilde{\mathbf{D}}_\Delta \tilde{\mathbf{D}}^{-1}$. Hence,

$$\begin{aligned} \mathbf{P}_{S_h} - \tilde{\mathbf{D}}^{-1} \mathbf{P}_0 &= \mathbf{P}_{S_h} - \mathbf{P}_S^e \tilde{\mathbf{D}}^{-1} \mathbf{P}_0 = \mathbf{P}_{S_h} - \mathbf{P}_S^e \mathbf{P}_0 + \mathbf{P}_S^e \tilde{\mathbf{D}}_\Delta \tilde{\mathbf{D}}^{-1} \mathbf{P}_0 \\ &= \mathbf{P}_{S_h} - \mathbf{P}_S^e + \mathbf{P}_S^e (\mathbf{I} - \mathbf{P}_0) + \mathbf{P}_S^e \tilde{\mathbf{D}}_\Delta \tilde{\mathbf{D}}^{-1} \mathbf{P}_0. \end{aligned} \quad (5.19)$$

From (5.10) we get $\|\mathbf{P}_{S_h} - \mathbf{P}_S^e\|_{L^\infty(S_h^n)} \lesssim h^{k_{g,s}} + \Delta t^{k_{g,q}}$ and $\|\mathbf{P}_S^e (\mathbf{I} - \mathbf{P}_0)\|_{L^\infty(S_h^n)} = \left\| \frac{\mathbf{P}_S \mathbf{n}_{S_h} \mathbf{n}_0^T}{\mathbf{n}_{S_h}^T \mathbf{n}_0} \right\|_{L^\infty(S_h^n)} \lesssim h^{k_{g,s}} + \Delta t^{k_{g,q}}$. With $\det(\tilde{\mathbf{D}}) = (\alpha^e)^2 \det(\mathbf{I} - \delta \mathbf{H})$ and the definition of $\tilde{\mathbf{D}}$ it follows that (for h and Δt sufficiently small) $\|\tilde{\mathbf{D}}^{-1}\|_{L^\infty(S_h^n)} \lesssim 1$. With (5.8) we get $\|\tilde{\mathbf{D}}_\Delta\|_{L^\infty(S_h^n)} \lesssim h^{k_{g,s}+1} + \Delta t^{k_{g,q}+1}$. Hence, $\left\| \mathbf{P}_S^e \tilde{\mathbf{D}}_\Delta \tilde{\mathbf{D}}^{-1} \mathbf{P}_0 \right\|_{L^\infty(S_h^n)} \lesssim h^{k_{g,s}+1} + \Delta t^{k_{g,q}+1}$. Using these estimates in (5.19) we obtain

$$\left\| \mathbf{P}_{S_h} - \tilde{\mathbf{D}}^{-1} \mathbf{P}_0 \right\|_{L^\infty(S_h^n)} \lesssim h^{k_{g,s}} + \Delta t^{k_{g,q}}. \quad (5.20)$$

Combining this with the result in (5.18) completes the proof. \square

The following corollary will be used in the consistency error analysis in Section 7.2. Let $\mathbf{v}_h : S_h \rightarrow \mathbb{R}^4$ be a vector-valued function with components given by $\mathbf{v}_h = (v_{h,i})$, $1 \leq i \leq 4$, and its surface gradient $\nabla_{S_h} \mathbf{v}_h = (\nabla_{S_h} v_{h,1}, \dots, \nabla_{S_h} v_{h,4})^T$.

COROLLARY 5.8. *For all $\mathbf{v}_h \in (W^{1,\infty}(S_h^n))^4$ the following uniform estimate holds:*

$$\left\| \operatorname{div}_{S_h} \mathbf{v}_h - (\operatorname{div}_S \mathbf{v}_h^l)^e \right\|_{L^\infty(S_h^n)} \lesssim (h^{k_{g,s}} + \Delta t^{k_{g,q}}) \|\nabla_{S_h} \mathbf{v}_h\|_{L^\infty(S_h^n)}. \quad (5.21)$$

Proof. Note that $\operatorname{div}_{S_h} \mathbf{v}_h = \operatorname{tr}(\mathbf{P}_{S_h} \nabla_{(x,t)} \mathbf{v}_h \mathbf{P}_{S_h}) = \operatorname{tr}(\nabla_{S_h} \mathbf{v}_h)$. Component-wise application of (5.18) yields

$$\operatorname{div}_{S_h} \mathbf{v}_h - (\operatorname{div}_S \mathbf{v}_h^l)^e = \operatorname{tr}(\nabla_{S_h} \mathbf{v}_h (\mathbf{P}_{S_h} - \tilde{\mathbf{D}}^{-1} \mathbf{P}_0)^T).$$

The result (5.21) follows using (5.20). \square

Choice of α_h . In Theorem 4.7 we used a general function α_h . For the formula (4.21) to be a discrete analogon of (4.16) we choose an α_h that approximates the function $\alpha = (1 + V^2)^{\frac{1}{2}}$. A natural choice for this approximation seems $\alpha_h = (1 + V_h^2)^{\frac{1}{2}}$, which has accuracy $\mathcal{O}(h^{k_{g,s}} + \Delta t^{k_{g,q}})$, cf. Remark 5.5. In the application that we consider below (Section 6) this approximation turns out to be *not* sufficiently accurate for an optimal order discretization error. We now introduce a (natural) specific choice for α_h which has an order of accuracy that is one higher than for $(1 + V_h^2)^{\frac{1}{2}}$. Let $\tilde{\phi}_h \in V_h^{k_{g,s}+1, k_{g,q}+1}$ be a one order higher order approximation of the level set function ϕ than the one introduced in Assumption 5.1. More precisely, we assume an approximation $\tilde{\phi}_h \in V_h^{k_{g,s}+1, k_{g,q}+1}$ of ϕ that satisfies for all $1 \leq n \leq N$ and $(m_s, m_q) \in (\{0, \dots, k_{g,s} + 1\} \times \{0, 1\}) \cup (\{0\} \times \{0, \dots, k_{g,q} + 1\})$

$$\|D^{m_s} \partial_t^{m_q} (\tilde{\phi}_h - \phi)\|_{L^\infty(\mathcal{T}_n^\Gamma \times I_n)} \lesssim h^{k_{g,s}+2-m_s} + \Delta t^{k_{g,q}+2-m_q}. \quad (5.22)$$

We define

$$\alpha_h := \sqrt{1 + \tilde{V}_h^2}, \quad \text{with } \tilde{V}_h := -\frac{\partial \tilde{\phi}_h}{\partial t} \left\| \nabla \tilde{\phi}_h \right\|^{-1}. \quad (5.23)$$

Note that the function \tilde{V}_h does not use the mesh deformation and is an approximation of order $\mathcal{O}(h^{k_{g,s}+1} + \Delta t^{k_{g,q}+1})$ of the normal velocity $V = \mathbf{w} \cdot \mathbf{n}$.

This choice for α_h is used in the remainder of this work.

A very similar one is used in the numerical experiments in [23]. The accuracy estimates (5.22) imply

$$\|\alpha^e - \alpha_h\|_{L^\infty(S_h)} \lesssim h^{k_{g,s}+1} + \Delta t^{k_{g,q}+1}, \quad (5.24)$$

$$\left\| \sqrt{1 + V_h^2} - \alpha_h \right\|_{L^\infty(S_h)} \lesssim h^{k_{g,s}} + \Delta t^{k_{g,q}}, \quad (5.25)$$

$$\left\| \nabla_{(\mathbf{x}, t)} (\alpha^e - \alpha_h) \right\|_{L^\infty(K_S)} \lesssim h^{k_{g,s}} + \Delta t^{k_{g,q}}, \quad K_S \in \mathcal{T}_{S_h}, \quad (5.26)$$

$$\left\| \mathbf{P}_S^e [\alpha_h^{-1}]_{\nu|F} \right\|_{L^\infty(F)} \lesssim h^{k_{g,s}+1} + \Delta t^{k_{g,q}+1}, \quad F \in \mathcal{F}. \quad (5.27)$$

The result (5.27) follows from (5.24), $[\alpha^e]_{\nu|F} = 0$ and the estimate (5.15). We finally derive an estimate for $R = \frac{1}{\alpha_h} \mathbf{w}_S \cdot \mathbf{n}_\partial$, with $\mathbf{n}_\partial = \frac{1}{\sqrt{1+V_h^2}} (V_h \mathbf{n}_h^T, 1)^T$, which appears in the partial integration formula in Theorem 4.7.

LEMMA 5.9. *The following estimate holds:*

$$\|R - 1\|_{L^\infty(S_h)} \lesssim h^{k_{g,s}} + \Delta t^{k_{g,q}}. \quad (5.28)$$

Proof. Note the estimate $\|\mathbf{w}^e \cdot \mathbf{n} - V_h\|_{L^\infty(S_h)} \lesssim h^{k_{g,s}} + \Delta t^{k_{g,q}}$, which follows from (5.10) and Lemma 4.4. From (5.8) and the smoothness of \mathbf{w} we get $\|\mathbf{w}_S - \mathbf{w}_S^e\|_{L^\infty(S_h)} \lesssim h^{k_{g,s}+1} + \Delta t^{k_{g,q}+1}$. Using this, (5.25) and (5.9) yields

$$\begin{aligned} \|R - 1\|_{L^\infty(S_h)} &= \left\| \frac{\mathbf{w}_S \cdot \mathbf{n}_\partial}{\alpha_h} - 1 \right\|_{L^\infty(S_h)} \lesssim \|\mathbf{w}_S^e \cdot \mathbf{n}_\partial - \alpha_h\|_{L^\infty(S_h)} + h^{k_{g,s}+1} + \Delta t^{k_{g,q}+1} \\ &\lesssim \left\| V_h \mathbf{w}^e \cdot \mathbf{n}_h + 1 - (1 + V_h^2) \right\|_{L^\infty(S_h)} + h^{k_{g,s}} + \Delta t^{k_{g,q}} \\ &\lesssim \|\mathbf{w}^e \cdot \mathbf{n} - V_h\|_{L^\infty(S_h)} + h^{k_{g,s}} + \Delta t^{k_{g,q}} \lesssim h^{k_{g,s}} + \Delta t^{k_{g,q}}. \end{aligned}$$

□

6. Application to a surface diffusive transport equation. We consider a well-known basic model for convection and molecular diffusion of a surface species, cf. [13, 4, 9]. The conservation of mass principle combined with Fick's law for the diffusive flux leads to the parabolic surface partial differential equation

$$\begin{aligned} \dot{u} + u \operatorname{div}_\Gamma \mathbf{w} - \mu_d \Delta_\Gamma u &= f \quad \text{on } \Gamma(t), \quad t \in (0, T], \\ u(\cdot, 0) &= 0 \quad \text{on } \Gamma(0), \end{aligned} \quad (6.1)$$

for the scalar unknown function $u = u(\mathbf{x}, t)$. Here $\mu_d > 0$ denotes the constant diffusion coefficient and $\dot{u} = \frac{\partial u^e}{\partial t} + \mathbf{w} \cdot \nabla u^e$ the material derivative along the velocity field \mathbf{w} , cf. (4.15). To simplify the error analysis below, we assume that the right-hand side f is such that $\int_{\Gamma(t)} f \, ds = 0$, $t \in [0, T]$, holds. This condition is satisfied if (6.1) is the transformed variant of an equation as in (6.1) with a nonzero initial condition and a source term that is zero. From the assumption on f it follows that a solution u of (6.1) has the property $\int_{\Gamma(t)} u \, ds = 0$ for all $t \in [0, T]$, which mimics a mass conservation property.

We introduce a variational space-time formulation of (6.1). A well-posed weak variational formulation in a suitable broken Hilbert space W_b is studied in [20]. We do not specify this space here. Multiplying (6.1) by test functions and integrating over the space-time slabs S_n results in the following variational problem, with the usual notation $[v]^n := v_+^n - v_-^n \in L^2(\Gamma(t_n))$ and $[v]^0 = v_+^0$. For a given $f \in L^2(S)$ determine $u \in W^b$ such that

$$\begin{aligned} \sum_{n=1}^N B_n(u, v) &:= \sum_{n=1}^N \left[\int_{S_n} \frac{1}{\alpha} \dot{u} v \, d\sigma + \int_{S_n} \frac{1}{\alpha} (uv \operatorname{div}_\Gamma \mathbf{w} + \mu_d \nabla_\Gamma u \cdot \nabla_\Gamma v) \, d\sigma \right. \\ &\quad \left. + ([u]^{n-1}, v_+^{n-1})_{\Gamma(t_{n-1})} \right] = \int_S \frac{1}{\alpha} f v \, ds \, dt \quad \text{for all } v \in W^b. \end{aligned} \quad (6.2)$$

Instead of space-time surface integrals of the form $\int_{S_n} \frac{1}{\alpha} g \, d\sigma$ one can also use the double integral $\int_{t_{n-1}}^{t_n} \int_{\Gamma(t)} g \, ds \, dt$. We use the surface variant with $\int_{S_n} \frac{1}{\alpha} g \, d\sigma$ because in the error analysis of the discretization method, that we treat below, we apply partial integration on the space-time surface S_h^n , cf. Theorem 4.7.

REMARK 6.1. Using partial integration

$$\begin{aligned} &\int_{S_n} \frac{1}{\alpha} \dot{u} v \, d\sigma \\ &= - \int_{S_n} \frac{1}{\alpha} (u \dot{v} + uv \operatorname{div}_\Gamma \mathbf{w}) \, d\sigma + (u_-^n, v_-^n)_{\Gamma(t_n)} - (u_+^{n-1}, v_+^{n-1})_{\Gamma(t_{n-1})}, \end{aligned} \quad (6.3)$$

for $u, v \in C^1(S^n)$, the formulation in (6.2) can be written in different equivalent forms. The discretization method below will be based on the antisymmetric formulation in which the material derivative appears in the form $\int_{S_n} \frac{1}{2\alpha} (\dot{u}v - u\dot{v}) \, d\sigma$.

6.1. Space-time trace finite element discretization. In this section we introduce a fully discrete higher order space-time discretization of (6.2), similar to [23]. The method is based on the standard space-time tensor product finite element space $V_h^{k_s, k_q}$, cf. (3.1). To obtain a higher order feasible geometry approximation we combine this space with the parametric mapping (3.3) as follows. We consider the prisms that are cut by S_{lin} , i.e. prisms in Q_h^S (cf. Fig. 3.1), and apply the mesh deformation

to obtain the domains:

$$Q_{\Theta,n}^S := \Theta_h^n(Q_n^S), \quad n = 1, \dots, N, \quad Q_{\Theta}^S := \bigcup_{n=1}^N Q_{\Theta,n}^S.$$

We define the parametric finite element space

$$V_{h,\Theta}^{k_s,k_q} := \left\{ v_h : Q_{\Theta}^S \rightarrow \mathbb{R}(\mathbf{x}, t) \mapsto v_h(\Theta_h^n(\mathbf{x}, t)) \in V_h^{k_s,k_q}|_{Q_n^S}, n = 1, \dots, N \right\}. \quad (6.4)$$

We use degree k_s and k_q in space and time, respectively. These degrees may be different from the degrees $k_{g,s}$ and $k_{g,q}$ that are used in the parametric mapping Θ_h^n , cf. (3.3). We introduce the following bilinear form on the time slab S_h^n :

$$\begin{aligned} B_{h,n}(u, v) &:= \int_{S_h^n} \frac{1}{\alpha_h} \left(\frac{1}{2} \dot{u}v - \frac{1}{2} u\dot{v} + \frac{1}{2} uv \operatorname{div}_{\Gamma_h} \mathbf{w} + \mu_d \nabla_{\Gamma_h} u \cdot \nabla_{\Gamma_h} v \right) d\sigma_h \\ &\quad + \frac{1}{2} (R_-^n u_-^n, v_-^n)_{\Gamma_h^n(t_n)} + \frac{1}{2} (R_+^{n-1} u_+^{n-1}, v_+^{n-1})_{\Gamma_h^n(t_{n-1})} \\ &\quad - (R_+^{n-1} u_-^{n-1} \circ \Theta_h^{n-1} \circ (\Theta_h^n)^{-1}, v_+^{n-1})_{\Gamma_h^n(t_{n-1})}, \end{aligned} \quad (6.5)$$

and its sum

$$B_h(u, v) := \sum_{n=1}^N B_{h,n}(u, v). \quad (6.6)$$

In addition we use two stabilization terms. The first one is a variant of the so-called volume normal derivative stabilization [7, 1]:

$$s_1(u, v) := \xi_1 \int_{Q_{\Theta}^S} (\mathbf{n}_h \cdot \nabla u)(\mathbf{n}_h \cdot \nabla v) d(\mathbf{x}, t). \quad (6.7)$$

With the average $\bar{u}_h^n(t) := \int_{\Gamma_h^n(t)} u ds_h$ we define the second stabilization term

$$s_2(u, v) := \xi_2 \sum_{n=1}^N \int_{t_{n-1}}^{t_n} \bar{u}_h^n \bar{v}_h^n dt. \quad (6.8)$$

Based on the literature we take the parameter range

$$h \lesssim \xi_1 \lesssim h^{-1}. \quad (6.9)$$

The parameter range for ξ_2 is specified in (7.3) below. We add these stabilizations to the bilinear form:

$$B_h^{\text{stab}}(u, v) := B_h(u, v) + s_1(u, v) + s_2(u, v). \quad (6.10)$$

Before defining the fully discrete problem we need a suitable approximation of the right hand side f . We assume $f_h \in L^2(S_h)$ to be an approximation of the exact data f satisfying

$$\|f_h - \mu_h f^e\|_{L^2(S_h)} \lesssim (h^{k_{g,s}+1} + \Delta t^{k_{g,q}+1}) \|f\|_{L^2(S)}. \quad (6.11)$$

From the literature it is known how such a data approximation can be determined, see e.g. [22, Remark 4.43] or [7, Remark 5] in similar settings.

We now introduce the *space-time discrete variational problem*: Given a right-hand side $f_h \in L^2(S_h)$ that satisfies (6.11), determine $u_h \in V_{h,\Theta}^{k_s,k_q}$ such that

$$B_h^{\text{stab}}(u_h, v_h) = \int_{S_h} \frac{f_h v_h}{\sqrt{1 + V_h^2}} d\sigma_h \quad \text{for all } v_h \in V_{h,\Theta}^{k_s,k_q}. \quad (6.12)$$

In the discrete problem above we used the antisymmetric form of the material derivative, cf. Remark 6.1. An advantage of this form is that it almost immediately leads to a stability estimate in a reasonable norm, cf. Section 7.1. An extensive discussion of implementation aspects of this method is given in [23, Subsection 3.7]. Here we only briefly address a few points.

The use of the function R in the boundary terms in (6.5) is motivated by the partial integration formula (4.21) on B_h^n . These weights can be included in an implementation without significant additional computational costs. In the consistency error analysis below this weighting with R plays a key role. We are not able to derive optimal bounds if we replace R by 1 and use the (sharp) estimates in Lemma 5.9. On the other hand, so far in numerical experiments we observe optimal order convergence if we replace R by 1.

The factor $\Theta_h^{n-1} \circ (\Theta_h^n)^{-1}$ that appears in the last term in (6.5) is included to (weakly) transfer the solution from the previous time interval I_{n-1} to the current one I_n . We need such a transfer operator because the approximate surface may be *discontinuous* between time slabs, $\Gamma_h^n(t_{n-1}) \neq \Gamma_h^{n-1}(t_{n-1})$, cf. Remark 3.2.

The volume normal derivative stabilization $s_1(\cdot, \cdot)$ is a standard technique in trace or cut finite element methods that is used to control the effects of small cuts. The other stabilization term $s_2(\cdot, \cdot)$ is motivated by a Poincaré type inequality. For this we recall that for $t \in [0, T]$ there are constants $c_{P,1}(t) > 0$, $c_{P,2}(t)$ such that for all $u \in H^1(\Gamma(t))$ the inequality $\|\nabla_\Gamma u\|_{L^2(\Gamma(t))}^2 \geq c_{P,1}(t)\|u\|_{L^2(\Gamma(t))}^2 - c_{P,2}(t)(\int_{\Gamma(t)} u ds)^2$ holds. Using smoothness assumptions (to have uniformity in t of the constants) and suitable perturbation arguments (cf. [22, Theorem 5.16]) one obtains, for sufficiently smooth functions u on S_h^n , $n = 1, \dots, N$,

$$\|\nabla_{\Gamma_h} u\|_{L^2(S_h^n)}^2 \geq C_{P,1}\|u\|_{L^2(S_h^n)}^2 - C_{P,2} \int_{t_{n-1}}^{t_n} (\bar{u}_h^n)^2 dt, \quad (6.13)$$

with strictly positive and uniform (in the discretization parameters) constants $C_{P,1}$, $C_{P,2}$. In the analysis we have to control the second term on the right-hand side in (6.13). For that we need the stabilization term $s_2(\cdot, \cdot)$.

7. Discretization error analysis. In this section we present an error analysis for the space-time discretization method (6.12). Optimal error bounds for the case of bi-linear finite element approximations are presented in [22]. The analysis in this section applies also to the case of higher order (iso)parametric finite element spaces. It is well-known that in the analysis of finite element discretization methods on stationary or evolving surfaces the treatment of the geometric error, i.e., the error caused by the numerical approximation of the surface, is a key point. Typically the analysis of the corresponding consistency error is rather technical. In the setting of the space-time finite element method (6.12) one has to control the difference between quantities on S and the corresponding ones on S_h . For this the results derived in the Sections 4 and 5 are essential ingredients.

We start with assumptions that simplify both the analysis and the presentation. We restrict to the *isoparametric* case, in the sense that the polynomial degrees used in the geometry approximation (parametric mapping) are the same as the ones used in the finite element spaces, i.e., $k_{g,s} = k_s$ and $k_{g,q} = k_q$. To further simplify the presentation we take $k_s = k_q$. We avoid space-time grid anisotropies by assuming

$$\Delta t \sim h.$$

In the remainder of this section, as discretization parameters we use the mesh size h ($\sim \Delta t$) and the polynomial degree k_s ($= k_{g,s} = k_{g,q} = k_q$). For the isoparametric finite element space we use the simplified notation $V_{h,\Theta}^{k_s} = V_{h,\Theta}^{k_s,k_q}$.

In the subsections below we treat different components of the error analysis. These are the usual ones for an inconsistent finite element method, namely a stability estimate, consistency error estimates and interpolation error estimates. In Section 7.1 we derive a stability result and formulate a Strang lemma. The stability analysis is fairly straightforward, because the bilinear form in the discretization (6.12) is anti-symmetric with respect to the material derivative, which almost immediately leads to a stable method. In Section 7.2 we analyze consistency errors. In that section many results presented in the Sections 4-5 will be used. Finally in Section 7.3 we briefly address interpolation error estimates and derive the main result Theorem 7.8, in which an optimal discretization error bound for the method (6.12) is presented.

In the error analysis we use the natural norm

$$\begin{aligned} \|u\|_{h,\Theta}^2 &:= \|u\|_{L^2(S_h)}^2 + \|\nabla_{\Gamma_h} u\|_{L^2(S_h)}^2 + \xi_1 \|\mathbf{n}_h \cdot \nabla u\|_{L^2(Q_h^\delta)}^2 \\ &+ \|u_-^N\|_{L^2(\Gamma_h^N(t_N))}^2 + \sum_{n=1}^N \left\| [u]_h^{n-1} \right\|_{L^2(\Gamma_h^n(t_{n-1}))}^2. \end{aligned} \quad (7.1)$$

7.1. Stability estimate and Strang lemma. We derive an ellipticity estimate for the bilinear form B_h^{stab} in the $\|\cdot\|_{h,\Theta}$ -norm. Note that this norm does not contain time derivatives. When considering $B_h^{\text{stab}}(u, u)$, $u \in V_{h,\Theta}^{k_s}$, the terms with the time derivative vanish. Hence, in the stability analysis we do not need partial integration and we do not need bounds for the (geometric) error terms that appear in the formula (4.21). However, we do have to control the geometric errors in the time slab boundary terms in (6.5).

We start with an assumption that we need in the stability analysis.

ASSUMPTION 7.1. *We assume that there exists a constant $c_{\text{div}} > 0$ such that*

$$\frac{\text{div}_{\Gamma_h} \mathbf{w}}{\alpha_h} + c_\alpha \mu_d C_{P,1} \geq c_{\text{div}} \quad \text{a.e. on } S_h, \quad (7.2)$$

where $C_{P,1}$ is the constant of the Poincaré inequality (6.13) and $c_\alpha := \|\alpha_h\|_{L^\infty(S_h)}^{-1}$.

Note that for convection-diffusion problems assumptions of this type are often used in the analysis of finite element methods. For the stabilization parameter ξ_2 used in $s_2(\cdot, \cdot)$ we assume

$$\frac{\mu_d C_{P,2} c_\alpha}{2} \leq \xi_2 \lesssim h^{-1}, \quad (7.3)$$

with $C_{P,2}$ from the Poincaré inequality (6.13). We now introduce an estimate that is crucial in the stability analysis of trace and cut finite element methods. This estimate

essentially bounds the L^2 -norm of finite element functions on a small strip around the discrete surface by the sum of the L^2 -norm on the surface and the L^2 -norm of the normal derivative in the strip. For stationary surfaces such estimates are known in the literature, also for higher order finite element spaces, e.g. [7]. For the discrete space-time surface that we consider in this paper and the case $k_s = 1$ (bi-linear finite elements) a proof is given in [22]. We think that the arguments used in this literature can be extended to the higher order space-time case. A rigorous proof, however, requires a detailed technical analysis that we do not present here. Without proof we introduce the following claim.

PROPOSITION 7.2. *For $v_h \in V_{h,\Theta}^{k_s}$ the following uniform estimate holds:*

$$\|v_h\|_{L^2(Q_\Theta^s)}^2 \lesssim h \left(\|v_h\|_{L^2(S_h)}^2 + s_1(v_h, v_h) \right). \quad (7.4)$$

The estimate (7.4) can be used to show that (7.1) defines a norm. Using standard finite element trace estimates and (7.4) one obtains

$$h \sum_{F \in \mathcal{F}_I} \|v_h\|_{L^2(F)}^2 \lesssim \|v_h\|_{h,\Theta}^2, \quad (7.5)$$

$$h \sum_{n=1}^N \left\| v_{h,-}^n \right\|_{L^2(\Gamma_h^n(t_n))}^2 \lesssim \|v_h\|_{h,\Theta}^2, \quad (7.6)$$

$$h \sum_{n=1}^N \left\| v_{h,+}^{n-1} \right\|_{L^2(\Gamma_h^n(t_{n-1}))}^2 \lesssim \|v_h\|_{h,\Theta}^2. \quad (7.7)$$

THEOREM 7.3. *There exists $c_s > 0$ such that for sufficiently small $h > 0$ the following ellipticity estimate holds:*

$$\inf_{u \in V_{h,\Theta}^{k_s}} \frac{B_h^{\text{stab}}(u, u)}{\|u\|_{h,\Theta}^2} \geq c_s. \quad (7.8)$$

Proof. For $k_s = 1$ a proof is given in [22, Theorem 5.19]. We assume $k_s > 1$. We note that for $k_s > 1$ the proof is simpler than for $k_s = 1$ because we can benefit from smaller perturbation terms $\|R - 1\|_{L^\infty(S_h)} \lesssim h^{k_s}$, cf. Lemma 5.9. We take an arbitrary $u \in V_{h,\Theta}^{k_s}$, $u \neq 0$. By definition we have

$$\begin{aligned} B_h^{\text{stab}}(u, u) &= \underbrace{\sum_{n=1}^N \int_{S_h^n} \frac{1}{2\alpha_h} \left(u^2 \operatorname{div}_{\Gamma_h} \mathbf{w} + 2\mu_d \nabla_{\Gamma_h} u \cdot \nabla_{\Gamma_h} u \right) d\sigma_h}_{F_1} + s_2(u, u) \\ &+ \sum_{n=1}^N \left[\frac{1}{2} (R_-^n u_-^n, u_-^n)_{\Gamma_h^n(t_n)} + \frac{1}{2} (R_+^{n-1} u_+^{n-1}, u_+^{n-1})_{\Gamma_h^n(t_{n-1})} \right. \\ &\quad \left. - (R_+^{n-1} u_-^{n-1} \circ \Theta_h^{n-1} \circ (\Theta_h^n)^{-1}, u_+^{n-1})_{\Gamma_h^n(t_{n-1})} \right] + s_1(u, u) \\ &=: F_1 + F_2 + s_1(u, u). \end{aligned} \quad (7.9)$$

For the term F_1 we use the Poincaré inequality (6.13) and the choice of ξ_2 (7.3) in

the stabilization term $s_2(u, u)$:

$$\begin{aligned} & \sum_{n=1}^N \left[\int_{S_h^n} \frac{1}{2\alpha_h} \left(u^2 \operatorname{div}_{\Gamma_h} \mathbf{w} + 2\mu_d \nabla_{\Gamma_h} u \cdot \nabla_{\Gamma_h} u \right) d\sigma_h \right] + s_2(u, u) \\ & \geq \sum_{n=1}^N \left[\frac{c_\alpha \mu_d}{2} \|\nabla_{\Gamma_h} u\|_{L^2(S_h^n)}^2 + \int_{S_h^n} \frac{1}{2} \left(\frac{1}{\alpha_h} \operatorname{div}_{\Gamma_h} \mathbf{w} + c_\alpha \mu_d C_{P,1} \right) u^2 d\sigma_h \right] \end{aligned}$$

Using the assumption (7.2) we then obtain

$$F_1 \geq \frac{1}{2} \min\{\mu_d c_\alpha, c_{\operatorname{div}}\} (\|u\|_{L^2(S_h)}^2 + \|\nabla_{\Gamma_h} u\|_{L^2(S_h)}^2). \quad (7.10)$$

We now treat the term F_2 . We use the notation $T_\Theta^{n-1} := \Theta_h^{n-1} \circ (\Theta_h^n)^{-1} : \Gamma_h^n(t_{n-1}) \rightarrow \Gamma_h^{n-1}(t_{n-1})$. Let $J_\Theta^{n-1} := \det(DT_\Theta^{n-1})$ denote the corresponding Jacobian determinant and

$$\tilde{F}_2 := \sum_{n=1}^N \left[\frac{1}{2} \|u_-^n\|_{L^2(\Gamma_h^n(t_n))}^2 + \frac{1}{2} \|u_+^{n-1}\|_{L^2(\Gamma_h^n(t_{n-1}))}^2 - \left(u_-^{n-1} \circ T_\Theta^{n-1}, u_+^{n-1} \right)_{\Gamma_h^n(t_{n-1})} \right]$$

the term F_2 with all R -terms replaced by 1. Using $\|R-1\|_{L^\infty(S_h)} \lesssim h^2$ and (7.6)-(7.7) we get

$$|F_2 - \tilde{F}_2| \lesssim h \|u\|_{h, \Theta}^2. \quad (7.11)$$

We further consider \tilde{F}_2 . Recall the jump term (4.19) across $\Gamma_h(t_{n-1})$: $[u]_h^{n-1} = u_+^{n-1} - u_-^{n-1} \circ T_\Theta^{n-1}$. Hence,

$$\begin{aligned} - \left(u_-^{n-1} \circ T_\Theta^{n-1}, u_+^{n-1} \right)_{\Gamma_h^n(t_{n-1})} &= -\frac{1}{2} \|u_-^{n-1} \circ T_\Theta^{n-1}\|_{L^2(\Gamma_h^n(t_{n-1}))}^2 \\ &\quad - \frac{1}{2} \|u_+^{n-1}\|_{L^2(\Gamma_h^n(t_{n-1}))}^2 + \frac{1}{2} \|[u]_h^{n-1}\|_{L^2(\Gamma_h^n(t_{n-1}))}^2. \end{aligned} \quad (7.12)$$

We now relate $\|u_-^{n-1} \circ T_\Theta^{n-1}\|_{L^2(\Gamma_h^n(t_{n-1}))}^2$ to $\|u_-^{n-1}\|_{L^2(\Gamma_h^{n-1}(t_{n-1}))}^2$:

$$\|u_-^{n-1}\|_{L^2(\Gamma_h^{n-1}(t_{n-1}))}^2 = \int_{\Gamma_h^{n-1}(t_{n-1})} (u_-^{n-1})^2 ds = \int_{\Gamma_h^n(t_{n-1})} (u_-^{n-1} \circ T_\Theta^{n-1})^2 |J_\Theta^{n-1}| ds.$$

Using (5.6) we get

$$\begin{aligned} & \max_{K \in \mathcal{T}_n^\Gamma} \left\| D\Theta_h^n(\cdot, t_n) D\Theta_h^{n+1}(\cdot, t_n)^{-1} - I \right\|_{L^\infty(K)} \\ & \lesssim \max_{K \in \mathcal{T}_n^\Gamma} \left\| D\Theta_h^n(\cdot, t_n) - D\Theta_h^{n+1}(\cdot, t_n) \right\|_{L^\infty(K)} \\ & = \max_{K \in \mathcal{T}_n^\Gamma} \left\| (D\Theta_h^n(\cdot, t_n) - D\Psi(\cdot, t_n)) + (D\Psi(\cdot, t_n) - D\Theta_h^{n+1}(\cdot, t_n)) \right\|_{L^\infty(K)} \lesssim h^{k_s} \lesssim h^2, \end{aligned}$$

and thus $|J_\Theta^{n-1} - 1| \lesssim h^2$. This yields (for h small enough)

$$\left| \|u_-^{n-1} \circ T_\Theta^{n-1}\|_{L^2(\Gamma_h^n(t_{n-1}))}^2 - \|u_-^{n-1}\|_{L^2(\Gamma_h^{n-1}(t_{n-1}))}^2 \right| \lesssim h^2 \|u_-^{n-1}\|_{L^2(\Gamma_h^{n-1}(t_{n-1}))}^2.$$

We use this in (7.12) and substitute in the expression for \tilde{F}_2 . This yields

$$\tilde{F}_2 \geq \frac{1}{2} \|u_-^N\|_{L^2(\Gamma_h^N(t_N))}^2 + \frac{1}{2} \sum_{n=1}^N \|[u]_h^{n-1}\|_{L^2(\Gamma_h^n(t_{n-1}))}^2 - ch^2 \sum_{n=1}^N \|u_-^{n-1}\|_{L^2(\Gamma_h^{n-1}(t_{n-1}))}^2,$$

with a suitable $c > 0$. Combining this with (7.6) and (7.11) we get

$$F_2 \geq \frac{1}{2} \|u_-^N\|_{L^2(\Gamma_h^N(t_N))}^2 + \frac{1}{2} \sum_{n=1}^N \|[u]_h^{n-1}\|_{L^2(\Gamma_h^n(t_{n-1}))}^2 - ch \|u\|_{h,\Theta}^2. \quad (7.13)$$

Combining the estimates for F_1 and F_2 and noting that $s_1(u, u)$ forms part of $\|u\|_{h,\Theta}^2$ we obtain

$$B_h^{\text{stab}}(u, u) \geq \frac{1}{2} \min\{\mu_d c_\alpha, c_{\text{div}}, 1\} \|u\|_{h,\Theta}^2 - ch \|u\|_{h,\Theta}^2.$$

Hence, for $h > 0$ sufficiently small we obtain the ellipticity estimate (7.8). \square

For the formulation of the Strang lemma we use an interpolation operator in the volume space-time finite element space denoted by $I_\Theta^{k_s} : C^0(Q_\Theta^S) \rightarrow V_{h,\Theta}^{k_s}$.

LEMMA 7.4. *Let $u \in H^2(S)$ be the solution of (6.2) and u_h the solution of (6.12). The following estimate holds.*

$$\begin{aligned} \|u^e - u_h\|_{h,\Theta} &\leq \|u^e - I_\Theta^{k_s}(u^e)\|_{h,\Theta} + c \sup_{v_h \in V_{h,\Theta}^{k_s}} \frac{B_h^{\text{stab}}(u^e - I_\Theta^{k_s}(u^e), v_h)}{\|v_h\|_{h,\Theta}} \\ &\quad + c \sup_{v_h \in V_{h,\Theta}^{k_s}} \frac{B_h^{\text{stab}}(u^e - u_h, v_h)}{\|v_h\|_{h,\Theta}}. \end{aligned} \quad (7.14)$$

Proof. This follows using a standard argument. By the triangle inequality and the ellipticity estimate (7.8) we have

$$\begin{aligned} \|u^e - u_h\|_{h,\Theta} &\leq \|u^e - I_\Theta^{k_s}(u^e)\|_{h,\Theta} + c \sup_{v_h \in V_{h,\Theta}^{k_s}} \frac{B_h^{\text{stab}}(u_h - I_\Theta^{k_s}(u^e), v_h)}{\|v_h\|_{h,\Theta}} \\ &\leq \|u^e - I_\Theta^{k_s}(u^e)\|_{h,\Theta} \\ &\quad + c \left(\sup_{v_h \in V_{h,\Theta}^{k_s}} \frac{B_h^{\text{stab}}(u^e - I_\Theta^{k_s}(u^e), v_h)}{\|v_h\|_{h,\Theta}} + \sup_{v_h \in V_{h,\Theta}^{k_s}} \frac{B_h^{\text{stab}}(u^e - u_h, v_h)}{\|v_h\|_{h,\Theta}} \right). \end{aligned}$$

\square

Estimates for the first term in the bound in (7.14) can be based on fairly straightforward interpolation error bounds. Such interpolation error bounds combined with a suitable continuity argument lead to an estimate for the second term on the right-hand side in (7.14), too. These estimates are further discussed in Section 7.3. In Section 7.2 we derive an estimate of the remaining third term, which measures the inconsistency due to geometric errors. Note that in case of an exact surface, i.e., $S_h = S$ and the finite element space $V_{h,\Theta}^{k_s}$ replaced by $V_h^{k_s}$ this term vanishes due to Galerkin orthogonality.

7.2. Consistency error analysis. The most technical part of the discretization error analysis is the derivation of bounds for the consistency error (third term of the right-hand side in (7.14)), which measures the effect of the geometry approximation. In this section we derive such bounds. We will use key results derived in the Sections 4 and 5, e.g., the partial integration rule (4.21) and the geometric estimates in the Lemmas 5.3, 5.6 and 5.9.

We start with two estimates that we use in the proof of Theorem 7.6 below.

LEMMA 7.5. *The following uniform estimates hold*

$$\left\| \operatorname{div}_{S_h} \left(\frac{1}{\alpha_h} \mathbf{P}_{S_h} \mathbf{w}_S \right) - \left(\operatorname{div}_S \frac{1}{\alpha} \mathbf{w}_S \right)^e \right\|_{L^\infty(S_h)} \lesssim h^{k_s}, \quad (7.15)$$

$$\left\| \operatorname{div}_{\Gamma_h} (\mathbf{w}^e) - \left(\operatorname{div}_\Gamma \mathbf{w} \right)^e \right\|_{L^\infty(S_h)} \lesssim h^{k_s}. \quad (7.16)$$

Proof. We write

$$\begin{aligned} & \operatorname{div}_{S_h} \left(\frac{1}{\alpha_h} \mathbf{P}_{S_h} \mathbf{w}_S \right) - \left(\operatorname{div}_S \frac{1}{\alpha} \mathbf{w}_S \right)^e = \\ & \left(\operatorname{div}_{S_h} \left(\frac{1}{\alpha_h} \mathbf{P}_{S_h} \mathbf{w}_S \right) - \operatorname{div}_{S_h} \frac{1}{\alpha^e} \mathbf{w}_S^e \right) + \left(\operatorname{div}_{S_h} \frac{1}{\alpha^e} \mathbf{w}_S^e - \left(\operatorname{div}_S \frac{1}{\alpha} \mathbf{w}_S \right)^e \right) = I + II. \end{aligned}$$

For the term II we use (5.21) with $\mathbf{v}_h = \frac{1}{\alpha^e} \mathbf{w}_S^e$, i.e., $\mathbf{v}_h^l = \frac{1}{\alpha} \mathbf{w}_S$, and thus we get

$$\left\| \operatorname{div}_{S_h} \frac{1}{\alpha^e} \mathbf{w}_S^e - \left(\operatorname{div}_S \frac{1}{\alpha} \mathbf{w}_S \right)^e \right\|_{L^\infty(S_h)} \lesssim h^{k_s}.$$

For term I we obtain, using the product rule, (5.26) and $\left\| \operatorname{div}_{S_h} (\mathbf{w}_S - \mathbf{w}_S^e) \right\|_{L^\infty(S_h)} \lesssim h^{k_s}$:

$$\begin{aligned} & \left\| \operatorname{div}_{S_h} \left(\frac{1}{\alpha_h} \mathbf{P}_{S_h} \mathbf{w}_S \right) - \operatorname{div}_{S_h} \frac{1}{\alpha^e} \mathbf{w}_S^e \right\|_{L^\infty(S_h)} \\ & \lesssim \left\| \operatorname{div}_{S_h} \left(\frac{1}{\alpha^e} (\mathbf{P}_{S_h} \mathbf{w}_S - \mathbf{w}_S^e) \right) \right\|_{L^\infty(S_h)} + h^{k_s} \lesssim \left\| \operatorname{div}_{S_h} (\mathbf{n}_{S_h} \mathbf{n}_{S_h} \cdot \mathbf{w}_S) \right\|_{L^\infty(S_h)} + h^{k_s} \\ & \lesssim \left\| \mathbf{n}_{S_h} \cdot \mathbf{w}_S \right\|_{L^\infty(S_h)} \left\| \operatorname{div}_{S_h} \mathbf{n}_{S_h} \right\|_{L^\infty(S_h)} + h^{k_s} \lesssim h^{k_s}. \end{aligned}$$

The second last inequality follows from the product rule for the divergence operator and by noting that $\mathbf{n}_{S_h}^T \nabla_{S_h} (\mathbf{n}_{S_h} \cdot \mathbf{w}_S) = 0$. In the last inequality we used $\mathbf{n}_{S_h} \cdot \mathbf{w}_S = \mathbf{P}_{S_h}^e \mathbf{n}_{S_h} \cdot \mathbf{w}_S$ and the estimate (5.10). A proof of (7.16) follows with similar arguments as in the proof of Corollary 5.8, using the transformation formula (4.22). \square

THEOREM 7.6. *Let $u \in H^2(S)$, $u \in H^1(\Gamma(t))$ for all $t \in [0, T]$, be the solution of (6.2) and u_h the solution of (6.12) with f_h that satisfies (6.11). Then we have the bound*

$$\sup_{v_h \in V_{h,\Theta}^{k_s}} \frac{|B_h^{\text{stab}}(u^e - u_h, v_h)|}{\|v_h\|_{h,\Theta}} \lesssim h^{k_s} (\|u\|_{H^2(S)} + h\|f\|_{L^2(S)}). \quad (7.17)$$

Proof. Let $v_h \in V_{h,\Theta}^{k_s}$ be arbitrary. First note that using $\mu_h \, ds_h = ds \circ \mathbf{p}$ we get the relation

$$B_h^{\text{stab}}(u_h, v_h) = \sum_{n=1}^N \int_{t_{n-1}}^{t_n} \int_{\Gamma_h^n(t)} (f_h - \mu_h f^e) v_h \, ds_h \, dt + \int_0^T \int_{\Gamma(t)} f v_h^l \, ds \, dt. \quad (7.18)$$

The function u solves the continuous problem (6.2), i.e. we have

$$\int_0^T \int_{\Gamma(t)} f v_h^l \, ds \, dt = \sum_{n=1}^N \left[\int_{S^n} \frac{1}{\alpha} \left(\dot{u} v_h^l + u v_h^l \operatorname{div}_{\Gamma} \mathbf{w} + \mu_d \nabla_{\Gamma} u \cdot \nabla_{\Gamma} v_h^l \right) d\sigma \right].$$

Note that $u \in C^0(S)$, hence the jump term in (6.2) vanishes. Note that $\dot{u} = \mathbf{w}_S \cdot \nabla_S u$. We use the results (4.13), (4.24) and (4.26) to transform back to the discrete manifold S_h , i.e.,

$$\begin{aligned} \int_0^T \int_{\Gamma(t)} f v_h^l \, ds \, dt &= \sum_{n=1}^N \left[\int_{S_h^n} \frac{\mu_h}{\sqrt{1+V_h^2}} (\mathbf{w}_S^e \cdot \tilde{\mathbf{D}}^{-1} \mathbf{P}_0 \nabla_{S_h} u^e) v_h \right. \\ &\quad \left. + \frac{\mu_h}{\sqrt{1+V_h^2}} u^e v_h (\operatorname{div}_{\Gamma} \mathbf{w})^e + \mu_d \mathbf{A}_h \nabla_{\Gamma_h} u^e \cdot \nabla_{\Gamma_h} v_h \, d\sigma_h \right]. \end{aligned} \quad (7.19)$$

On the other hand, for the (extended) exact solution u^e substituted in the discrete bilinear form (6.10) we obtain

$$\begin{aligned} B_h^{\text{stab}}(u^e, v_h) &= \sum_{n=1}^N \left[\int_{S_h^n} \frac{1}{2\alpha_h} (v_h \dot{u}^e - u^e \dot{v}_h + u^e v_h \operatorname{div}_{\Gamma_h} \mathbf{w} + 2\mu_d \nabla_{\Gamma_h} u^e \cdot \nabla_{\Gamma_h} v_h) \, d\sigma_h \right. \\ &\quad + \frac{1}{2} \int_{\Gamma_h^n(t_n)} u^e v_{h,-}^{n-1} R_-^{n-1} \, ds_h + \frac{1}{2} \int_{\Gamma_h^n(t_{n-1})} u^e v_{h,+}^{n-1} R_+^{n-1} \, ds_h \\ &\quad \left. - \int_{\Gamma_h^n(t_{n-1})} (u^e \circ \Theta_h^{n-1} \circ (\Theta_h^n)^{-1}) v_{h,+}^{n-1} R_+^{n-1} \, ds_h \right] + s_1(u^e, v_h) + s_2(u^e, v_h). \quad \blacksquare \end{aligned}$$

Partial integration (4.21) leads to

$$\begin{aligned} B_h^{\text{stab}}(u^e, v_h) &= \sum_{n=1}^N \left[\int_{S_h^n} \frac{1}{\alpha_h} (\dot{u}^e v_h + \frac{1}{2} u^e v_h \operatorname{div}_{\Gamma_h} \mathbf{w} + \mu_d \nabla_{\Gamma_h} u^e \cdot \nabla_{\Gamma_h} v_h) \, d\sigma_h \right. \\ &\quad + \int_{\Gamma_h^n(t_{n-1})} [u^e]_h^{n-1} v_{h,+}^{n-1} R_+^{n-1} \, ds_h + \frac{1}{2} \sum_{K_S \in \mathcal{T}_{S_h^n}} \int_{K_S} u^e v_h \operatorname{div}_{S_h} \left(\frac{1}{\alpha_h} \mathbf{P}_{S_h} \mathbf{w}_S \right) \, d\sigma_h \\ &\quad \left. - \frac{1}{2} \sum_{F \in \mathcal{F}_h^n} \int_F u^e v_h \mathbf{w}_S \cdot [\alpha_h^{-1}]_{\nu} \, dF \right] + s_1(u^e, v_h) + s_2(u^e, v_h). \end{aligned} \quad (7.20)$$

We combine (7.18)–(7.20) and obtain, using $u^\circ = \mathbf{w}_S \cdot \nabla_{S_h} u^e$,

$$B_h^{\text{stab}}(u^e - u_h, v_h) = \int_{S_h} \left(\frac{1}{\alpha_h} \mathbf{w}_S^T - \frac{\mu_h}{\sqrt{1+V_h^2}} \mathbf{w}_S^e \cdot \tilde{\mathbf{D}}^{-1} \mathbf{P}_0 \right) \nabla_{S_h} u^e v_h \, d\sigma_h \quad (7.21)$$

$$+ \underbrace{\int_{S_h} \frac{1}{2\alpha_h} u^e v_h \operatorname{div}_{\Gamma_h} \mathbf{w} - \frac{\mu_h}{\sqrt{1+V_h^2}} u^e v_h (\operatorname{div}_{\Gamma} \mathbf{w})^e \, d\sigma_h}_I$$

$$+ \mu_d \int_{S_h} \left(\frac{1}{\alpha_h} \mathbf{I} - \mathbf{A}_h \right) \nabla_{\Gamma_h} u^e \cdot \nabla_{\Gamma_h} v_h \, d\sigma_h \quad (7.22)$$

$$+ \sum_{n=1}^N \left[\int_{\Gamma_h^n(t_{n-1})} [u^e]_h^{n-1} v_{h,+}^{n-1} R_+^{n-1} \, ds_h \right] \quad (7.23)$$

$$+ \underbrace{\frac{1}{2} \sum_{K_S \in \mathcal{T}_{S_h}} \int_{K_S} u^e v_h \operatorname{div}_{S_h} \left(\frac{1}{\alpha_h} \mathbf{P}_{S_h} \mathbf{w}_S \right) \, d\sigma_h}_II - \underbrace{\frac{1}{2} \sum_{F \in \mathcal{F}_I} \int_F u^e v_h \mathbf{w}_S \cdot \mathbf{P}_S^e \left[\alpha_h^{-1} \right]_\nu \, dF}_{III}$$

$$+ \int_{S_h} \frac{(f_h - \mu_h f^e) v_h}{\sqrt{1+V_h^2}} \, d\sigma_h + s_1(u^e, v_h) + s_2(u^e, v_h). \quad (7.24)$$

We now derive bounds for these terms using results from Sections 4 and 5. We first consider the term on the right-hand side in (7.21), denoted by T_1 . Using the smoothness of \mathbf{w} , (5.12), (5.25) and (5.20) we get

$$\left\| \left(\frac{1}{\alpha_h} \mathbf{w}_S^T - \frac{\mu_h}{\sqrt{1+V_h^2}} \mathbf{w}_S^T \tilde{\mathbf{D}}^{-1} \mathbf{P}_0 \right) \mathbf{P}_{S_h} \right\|_{L^\infty(S_h)} \lesssim \left\| \mathbf{P}_{S_h} - \tilde{\mathbf{D}}^{-1} \mathbf{P}_0 \right\|_{L^\infty(S_h)} + h^{k_s} \lesssim h^{k_s}.$$

From this it follows that $|T_1| \lesssim h^{k_s} \|v_h\|_{L^2(S_h)} \|u\|_{H^1(S)}$. We now estimate the term in (7.22), denoted by T_2 . Recall the definition of \mathbf{A}_h in (4.23). We again use (5.12), (5.25). Also note that $(\mathbf{I} - \delta \mathbf{H})^{-1} = \mathbf{I} + \mathcal{O}(h^{k_s+1})$ and $\mathbf{P}_h \tilde{\mathbf{P}}_h = \mathbf{P}_h$. With these results we obtain

$$\left\| \left(\frac{1}{\alpha_h} \mathbf{I} - \mathbf{A}_h \right) \mathbf{P}_h \right\|_{L^\infty(S_h)} \lesssim \left\| \mathbf{P}_h - \tilde{\mathbf{P}}_h \right\|_{L^\infty(S_h)} + h^{k_s} \lesssim h^{k_s},$$

and with this we get $|T_2| \lesssim h^{k_s} \|v_h\|_{L^2(S_h)} \|u\|_{H^1(S)}$. We consider the term in (7.23), denoted by T_3 . Using the continuity of u^e we get, on $\Gamma_h^n(t_{n-1})$:

$$[u^e]_h^{n-1} = u^e (\operatorname{id} - \Theta_h^{n-1} \circ (\Theta_h^n)^{-1}) = u^e (\Theta_h^n - \Theta_h^{n-1}) (\Theta_h^n)^{-1}. \quad (7.25)$$

Using (5.5) and a Sobolev embedding estimate we obtain $\|[u^e]_h^{n-1}\|_{L^\infty(\Gamma_h^n(t_{n-1}))} \lesssim h^{k_s+1} \|u\|_{H^2(S)}$. Combining this with (7.7) yields

$$|T_3| \lesssim h^{k_s+1} \|u\|_{H^2(S)} \sum_{n=1}^N \left\| v_{h,+}^{n-1} \right\|_{L^2(\Gamma_h^n(t_{n-1}))}$$

$$\lesssim h^{k_s+\frac{1}{2}} \left(\sum_{n=1}^N \left\| v_{h,+}^{n-1} \right\|_{L^2(\Gamma_h^n(t_{n-1}))}^2 \right)^{\frac{1}{2}} \|u\|_{H^2(S)} \lesssim h^{k_s} \|v_h\|_{h,\Theta} \|u\|_{H^2(S)}. \quad (7.26)$$

We combine the terms (I) and (II). First note that using (7.16), (5.12), (5.25) and (5.24) we get

$$|(I) + \int_{S_h} \frac{1}{2\alpha^e} u^e v_h (\operatorname{div}_{\Gamma} \mathbf{w})^e \, d\sigma_h| \lesssim h^{k_s} \|u\|_{L^2(S)} \|v_h\|_{L^2(S_h)}.$$

Using (7.15) and (4.14) yields

$$\left| (II) - \int_{S_h} \frac{1}{2\alpha^e} u^e v_h (\operatorname{div}_\Gamma \mathbf{w})^e d\sigma_h \right| \lesssim h^{k_s} \|u\|_{L^2(S)} \|v_h\|_{L^2(S_h)}.$$

Combining this we obtain $|(I) + (II)| \lesssim h^{k_s} \|u\|_{L^2(S)} \|v_h\|_{L^2(S_h)}$.

We turn to the bound for (III). We need the following Hansbo trace type inequality. For an arbitrary $F \in \mathcal{F}_I$ we take a corresponding four-dimensional space-time prism P of the outer triangulation $P \in Q_h^S$ with $P \cap F \neq \emptyset$. We then have for $w \in H^2(P)$

$$\begin{aligned} \|w\|_{L^2(F)}^2 &\lesssim h^{-1} \|w\|_{L^2(\partial P)}^2 + h \|w\|_{H^1(\partial P)}^2 \\ &\lesssim h^{-2} \|w\|_{L^2(P)}^2 + \|w\|_{H^1(P)}^2 + h^2 \|w\|_{H^2(P)}^2, \end{aligned} \quad (7.27)$$

which follows from [10, Lemma 4.2]. Note that for $P \in Q_h^S$ we have $\|\delta\|_{L^\infty(P)} \lesssim h$ and using $\mathbf{n} \cdot \nabla u^e = 0$ on P we get [19, Section 6.1] $\|u^e\|_{H^2(P)}^2 \lesssim h \|u\|_{H^2(S \cap P)}^2$. With this, the bound of the conormal jumps in (5.27), the trace inequality (7.27) and the face integral bound (7.5) we obtain:

$$\begin{aligned} |(III)| &\lesssim h^{k_s+1} \left(\sum_{P \in Q_h^S} h^{-2} \|u^e\|_{L^2(P)}^2 + 2 \|u^e\|_{H^1(P)}^2 + h^2 \|u^e\|_{H^2(P)}^2 \right)^{\frac{1}{2}} \left(\sum_{F \in \mathcal{F}_I} \|v_h\|_{L^2(F)}^2 \right)^{\frac{1}{2}} \\ &\lesssim h^{k_s+1} \left(\sum_{P \in Q_h^S} h^{-2} \|u^e\|_{H^2(P)}^2 \right)^{\frac{1}{2}} \left(\sum_{F \in \mathcal{F}_I} \|v_h\|_{L^2(F)}^2 \right)^{\frac{1}{2}} \\ &\lesssim h^{k_s+1} h^{-\frac{1}{2}} \|u\|_{H^2(S)} h^{-\frac{1}{2}} \|v_h\|_{h,\Theta} \lesssim h^{k_s} \|u\|_{H^2(S)} \|v_h\|_{h,\Theta}. \end{aligned}$$

Finally we consider the terms in (7.24). For the first term in (7.24) we get, using the data accuracy assumption (6.11):

$$\left| \int_{S_h} \frac{(f_h - \mu_h f^e) v_h}{\sqrt{1 + V_h^2}} d\sigma_h \right| \lesssim h^{k_s+1} \|f\|_{L^2(S)} \|v_h\|_{L^2(S_h)}. \quad (7.28)$$

For the normal gradient stabilization term we use $\mathbf{n} \cdot \nabla u^e = 0$, (5.9) and $\|u^e\|_{H^2(Q^S)}^2 \lesssim h \|u\|_{H^2(S)}^2$:

$$\begin{aligned} |s_1(u^e, v_h)| &= \left| \xi_1 \int_{Q^S} (\mathbf{n}_h \cdot \nabla u^e) (\mathbf{n}_h \cdot \nabla v_h) d(\mathbf{x}, t) \right| \\ &= \left| \xi_1 \int_{Q^S} ((\mathbf{n} - \mathbf{n}_h) \cdot \nabla u^e) (\mathbf{n}_h \cdot \nabla v_h) d(\mathbf{x}, t) \right| \\ &\lesssim \xi_1^{\frac{1}{2}} h^{k_s} \|\nabla u^e\|_{L^2(Q^S)} \xi_1^{\frac{1}{2}} \|\mathbf{n}_h \cdot \nabla v_h\|_{L^2(Q^S)} \lesssim h^{k_s} \|u\|_{H^2(S)} \|v_h\|_{h,\Theta}. \end{aligned} \quad (7.29)$$

For the other stabilization term we use $\int_{\Gamma(t)} u ds = 0$, $\mu_h ds_h = ds$, the estimate (5.12), which then implies $|\overline{u^e}^n(t)| \lesssim h^{k_s+1} \|u\|_{L^2(\Gamma(t))}$. Using this and the upper bound for (7.3) for ξ_2 :

$$|s_2(u^e, v_h)| = \xi_2 \left| \sum_{n=1}^N \int_{t_{n-1}}^{t_n} \overline{u^e}^n \overline{v_h}^n dt \right| \lesssim h^{k_s} \|u\|_{L^2(S)} \|v_h\|_{L^2(S_h)}.$$

Combining the estimates for the different terms in (7.21)-(7.24) completes the proof. \square

7.3. Interpolation and discretization error bounds. In this section we discuss how bounds for the first and second term on the right-hand side of the Strang estimate (7.14) can be derived. These are based on interpolation error bounds and a continuity estimate. We first address the interpolation error bounds. The interpolation operator $I_{\Theta}^{k_s} : C^0(Q_{\Theta}^S) \rightarrow V_{h,\Theta}^{k_s}$ is defined by $(I_{\Theta}^{k_s} v) \circ \Theta_h^n = I^{k_s}(v \circ \Theta_h^n)$ on Q_n^S , with I^{k_s} the standard nodal interpolation operator in the space-time finite element space $V_h^{k_s}$ of polynomials of degree k_s both in space and in time. For I^{k_s} optimal error bounds are well-known. With fairly straightforward arguments, which are elaborated for the stationary case in [7] and for the space-time case with $k_s = 1$ in [22], one obtains optimal interpolation error bounds for $I_{\Theta}^{k_s}$, too.

PROPOSITION 7.7. *For $u \in H^{k_s+1}(S)$ we have*

$$\begin{aligned} & \|u^e - I_{\Theta}^{k_s}(u^e)\|_{L^2(Q_{\Theta}^S)} + h\|u^e - I_{\Theta}^{k_s}(u^e)\|_{H^1(Q_{\Theta}^S)} \\ & \lesssim h^{k_s+1}\|u^e\|_{H^{k_s+1}(Q_{\Theta}^S)} \lesssim h^{k_s+\frac{3}{2}}\|u\|_{H^{k_s+1}(S)}, \end{aligned} \quad (7.30)$$

$$\|u^e - I_{\Theta}^{k_s}(u^e)\|_{L^2(S_h)} + h\|u^e - I_{\Theta}^{k_s}(u^e)\|_{H^1(S_h)} \lesssim h^{k_s+1}\|u\|_{H^{k_s+1}(S)}, \quad (7.31)$$

and

$$\|u^e - I_{\Theta}^{k_s}(u^e)\|_{h,\Theta} \lesssim h^{k_s}\|u\|_{H^{k_s+1}(S)} + h^{k_s+\frac{1}{2}}\|u\|_{W^{1,\infty}(S)}. \quad (7.32)$$

Proof. We do not include a proof of (7.30)-(7.31). The first result can be derived using the relation between $I_{\Theta}^{k_s}$ and I^{k_s} and standard error bounds for the latter. The result (7.31) can be derived using (7.30) and an Hansbo type estimate as in (7.27). We outline how (7.32) can be derived using (7.30)-(7.31). Bounds for the first three terms in the norm $\|u^e - I_h(u^e)\|_{h,\Theta}$, cf. (7.1), immediately follow from (7.30)-(7.31). For the fourth term in this norm we apply the trace estimate $\|w\|_{L^2(\Gamma_h^N(t_N))} \lesssim \|w\|_{H^1(S_h)}$ and then use the result (7.31). We finally consider the last term in the norm $\|u^e - I_{\Theta}^{k_s}(u^e)\|_{h,\Theta}$ that measures the size of the jump term $[u^e - I_{\Theta}^{k_s}(u^e)]_h^{n-1}$ on $\Gamma_h^n(t_{n-1})$. We introduce notation $\hat{\Theta}_h^n := \Theta_h^n(\cdot, t_{n-1})$, $\hat{\Theta}_h^{n-1} := \Theta_h^{n-1}(\cdot, t_{n-1})$. Note that $\hat{\Theta}_h^n : \Gamma_{\text{lin}}(t_{n-1}) \rightarrow \Gamma_h^n(t_{n-1})$ is a bijection with inverse $(\hat{\Theta}_h^n)^{-1} = (\Theta_h^n)^{-1}(\cdot, t_{n-1})$. We denote the (nodal) interpolation error operators by $E_{\Theta}^{k_s} := I - I_{\Theta}^{k_s}$, $E^{k_s} := I - I^{k_s}$. Then we obtain, using the definition of $[\cdot]_h^{n-1}$, boundedness of the standard nodal interpolation operator in the maximum norm and (5.5):

$$\begin{aligned} & \| [E_{\Theta}^{k_s}(u^e)]_h^{n-1} \|_{L^2(\Gamma_h^n(t_{n-1}))} \lesssim \| [E_{\Theta}^{k_s}(u^e)]_h^{n-1} \circ \hat{\Theta}_h^n \|_{L^2(\Gamma_{\text{lin}}(t_{n-1}))} \\ & \lesssim \| E_{\Theta}^{k_s}(u^e) \circ \hat{\Theta}_h^n - E_{\Theta}^{k_s}(u^e) \circ \hat{\Theta}_h^{n-1} \|_{L^2(\Gamma_{\text{lin}}(t_{n-1}))} \\ & \lesssim \| E^{k_s}(u^e \circ \hat{\Theta}_h^n - u^e \circ \hat{\Theta}_h^{n-1}) \|_{L^\infty(\Omega_n^\Gamma|_{t=t_{n-1}})} \\ & \lesssim \| u^e \circ \hat{\Theta}_h^n - u^e \circ \hat{\Theta}_h^{n-1} \|_{L^\infty(\Omega_n^\Gamma|_{t=t_{n-1}})} \\ & \lesssim \| \nabla u^e \|_{L^\infty(\Omega_n^\Gamma|_{t=t_{n-1}})} h^{k_s+1} \lesssim h^{k_s+1} \| u \|_{W^{1,\infty}(S)}. \end{aligned} \quad (7.33)$$

Using (7.33), the last term in the norm $\|u^e - I_{\Theta}^{k_s}(u^e)\|_{h,\Theta}$ can be estimated by $h^{k_s+\frac{1}{2}}\|u\|_{W^{1,\infty}(S)}$. Combining these results we obtain the result (7.32). \square

As final step in the error analysis we have to derive a bound for the term $B_h^{\text{stab}}(u^e - I_{\Theta}^{k_s}(u^e), v_h)$ in the Strang estimate (7.14). For this we can use arguments very similar to ones used above. We outline the key steps. First we apply partial integration, as in the proof of Theorem 7.6, which results in the relation (7.20) with

u^e replaced by the interpolation error $E_{\Theta}^{k_s}(u^e) := u^e - I_{\Theta}^{k_s}(u^e)$. The first, second, third and fifth term on the right-hand side in (7.20) can be estimated using the Cauchy Schwarz inequality and the interpolation error bounds in (7.31), resulting in a bound $ch^{k_s}\|u\|_{H^{k_s+1}(S)}\|v_h\|_{h,\Theta}$. For the fourth term on the right-hand side in (7.20), with the jump term $[E_{\Theta}^{k_s}(u^e)]_h^{n-1}$, we use the estimates (7.33) and (7.7), which then results in a bound $ch^{k_s}\|u\|_{W^{1,\infty}(S)}\|v_h\|_{h,\Theta}$. The sixth term on the right-hand side in (7.20) contains the sum over the faces $F \in \mathcal{F}_I^n$. For the interpolation error on these faces $\|E_{\Theta}^{k_s}(u^e)\|_{L^2(F)}$ we use (7.27) and the interpolation error bound (7.30). Combining this with (7.5) results in a bound $ch^{k_s}\|u\|_{H^{k_s+1}(S)}\|v_h\|_{h,\Theta}$ for the sixth term. It remains to derive bounds for the stabilization terms $s_1(E_{\Theta}^{k_s}(u^e), v_h)$ and $s_2(E_{\Theta}^{k_s}(u^e), v_h)$. For the former one obtains with the Cauchy Schwarz inequality and (7.30) the estimate $|s_1(E_{\Theta}^{k_s}(u^e), v_h)| \lesssim h^{k_s}\|u\|_{H^{k_s+1}(S)}\|v_h\|_{h,\Theta}$. For the latter stabilization term we use repeated Cauchy-Schwarz and (7.31), which yields

$$|s_2(E_{\Theta}^{k_s}(u^e), v_h)| \lesssim h^{-1}\|E_{\Theta}^{k_s}(u^e)\|_{L^2(S_h)}\|v_h\|_{L^2(S_h)} \lesssim h^{k_s}\|u\|_{H^{k_s+1}(S)}\|v_h\|_{h,\Theta}.$$

Summarizing, we obtain for the remaining term in the Strang estimate (7.14) the bound

$$\sup_{v_h \in V_{h,\Theta}^{k_s}} \frac{B_h^{\text{stab}}(u_h - I_{\Theta}^{k_s}(u^e), v_h)}{\|v_h\|_{h,\Theta}} \lesssim h^{k_s} (\|u\|_{H^{k_s+1}(S)} + \|u\|_{W^{1,\infty}(S)}). \quad (7.34)$$

As a direct consequence of the Strang lemma 7.4 and the estimates derived in Theorem 7.6, Proposition 7.7 and (7.34) we obtain the following discretization error bound.

THEOREM 7.8. *For the solution u of (6.2) we assume $u \in H^{k_s+1}(S) \cap W^{1,\infty}(S)$. Let u_h be the solution of (6.12). The following discretization error estimate holds:*

$$\|u^e - u_h\|_{h,\Theta} \lesssim h^{k_s} (\|u\|_{H^{k_s+1}(S)} + \|u\|_{W^{1,\infty}(S)} + h\|f\|_{L^2(S)}). \quad (7.35)$$

REMARK 7.9. The energy norm $\|\cdot\|_{h,\Theta}$ contains a spatial gradient. Hence, for $\Delta t \sim h$ and using finite element polynomials of degree k_s in space and time, the interpolation error in this norm is of order $\mathcal{O}(h^{k_s})$. The discretization error bound (7.35) is optimal in the sense that it has the same order of convergence k_s . The bound confirms the convergence results obtained in numerical experiments with $k_s = 1, 2, 3, 4$, cf. [23]. One expects one order more if only the L^2 error (in space and time) is considered, cf. also the experiments in [23]. Such a result, however, has not been rigorously derived, yet.

The result in Theorem 7.8 is the first error bound for this type of higher order Eulerian space-time discretization method. The result, although sharp in the sense as explained above, is still very crude due to the assumptions $k_{g,s} = k_{g,q} = k_q = k_s$ and $\Delta t \sim h$. Several interesting accuracy issues are not addressed by our crude analysis. Here we mention two of these. If we keep the assumption $k_{g,s} = k_{g,q} = k_q = k_s$ but drop $\Delta t \sim h$ then, due to the fact that the energy norm does not contain a derivative with respect to t , for the interpolation error term in (7.14) we expect,

$$\|u^e - I_{\Theta}^{k_s}(u^e)\|_{h,\Theta} \lesssim h^{k_s} + \Delta t^{k_s+1},$$

cf. the interpolation error bounds in [11]. Such a higher order convergence with respect to Δt in the energy norm is, however, not observed in experiments. This might

be due to consistency error terms that contain derivatives also in time direction and for which the optimal bound is of order $h^{k_s} + \Delta t^{k_s}$, cf. (5.21). A rigorous theoretical explanation, however, is lacking. One other issue is related to the well-known super-convergence effect of DG time discretization methods at the nodes, cf. [24, Theorem 12.3]. We do not observe this effect in our numerical experiments. A satisfactory explanation for this is lacking.

Concerning mass conservation properties of the discrete scheme there is no rigorous analysis. Numerical experiments in [22, Section 6] and [23] show that the mass error $m(t) := |\int_{\Gamma_h^n(t)} u_h ds_h - \int_{\Gamma_h^0} u_h ds_h|$, $t \in I_n$, is essentially independent of n and for the case $k_{g,s} = k_s = k_{g,q} = k_q = 1$ and $\Delta t \sim h$ we observe $m(t) \sim h^2$.

Acknowledgement. The authors thank the German Research Foundation (DFG) for financial support within the Research Unit "Vector- and tensor valued surface PDEs" (FOR 3013) with project no. RE 1461/11-2.

8. Appendix: proof of Lemma 4.1. For $B \subset \mathbb{R}^3$ let $\mathbf{f} : B \rightarrow S_h^n$ be a local parametrization of S_h^n . The Lebesgue measure on B is denoted by $d\mathbf{z}$. The Jacobian of \mathbf{f} is denoted by $D_{\mathbf{z}}\mathbf{f} =: \mathbf{F} : B \rightarrow \mathbb{R}^{4 \times 3}$. The three columns of \mathbf{F} are tangential to S_h^n . For given $\mathbf{z} \in B$ we introduce a singular value decomposition $\mathbf{F} = \mathbf{U}\mathbf{\Sigma}\mathbf{V}^T$, with orthogonal matrices $\mathbf{U} = (\mathbf{u}_1, \mathbf{u}_2, \mathbf{u}_3, \mathbf{u}_4) \in \mathbb{R}^{4 \times 4}$ and $\mathbf{V} \in \mathbb{R}^{3 \times 3}$. The singular values are denoted by σ_i , $i = 1, 2, 3$. We choose \mathbf{u}_i , $1 \leq i \leq 4$, such that $\mathbf{u}_4(\mathbf{z}) = \mathbf{n}_{S_h}(\mathbf{f}(\mathbf{z}))$. We obtain

$$d\sigma_h = \sqrt{\det(\mathbf{F}^T \mathbf{F})} d\mathbf{z} = \sqrt{\det(\mathbf{V}\mathbf{\Sigma}^T \mathbf{U}^T \mathbf{U}\mathbf{\Sigma}\mathbf{V}^T)} d\mathbf{z} = \prod_{i=1}^3 \sigma_i d\mathbf{z}. \quad (8.1)$$

We write $\delta_t := \frac{\partial \delta}{\partial t}$ and $\mathbf{n}_t = \frac{\partial \mathbf{n}}{\partial t}$ on U and note that $\mathbf{n} \cdot \mathbf{n}_t = 0$ holds. A local parametrization of S^n is given by $\mathbf{p} \circ \mathbf{f} : B \rightarrow S^n$. Its Jacobian $\mathbf{A} := D_{\mathbf{z}}(\mathbf{p} \circ \mathbf{f}) : B \rightarrow \mathbb{R}^{4 \times 3}$ is given by

$$\mathbf{A} = \begin{pmatrix} \mathbf{P} - \delta \mathbf{H} & -\delta_t \mathbf{n} - \delta \mathbf{n}_t \\ 0 & 1 \end{pmatrix} \mathbf{F}.$$

For ease of presentation we omit function arguments, noting that the functions \mathbf{F} , \mathbf{U} , \mathbf{U}_m , \mathbf{V} , \mathbf{V}_m , $\mathbf{\Sigma}$, $\mathbf{\Sigma}_m$, σ_i , $d\mathbf{z}$, some of which are introduced below, are evaluated on B , while the other functions are evaluated, via composition with \mathbf{f} , on S_h^n . We obtain the surface measure relation $d\sigma = \sqrt{\det(\mathbf{A}^T \mathbf{A})} d\mathbf{z}$ and thus

$$\mu_h^S = \frac{\sqrt{\det(\mathbf{A}^T \mathbf{A})}}{\prod_{i=1}^3 \sigma_i}. \quad (8.2)$$

We will express $\det(\mathbf{A}^T \mathbf{A})$ in terms of the singular values σ_i using basic linear algebra relations. Using the Schur complement formula it follows that for $\mathbf{G} \in \mathbb{R}^{n \times (n-1)}$, $\mathbf{y} \in \mathbb{R}^n$, $\mathbf{y} \neq 0$, we have

$$\det \begin{pmatrix} \mathbf{G} & \mathbf{y} \end{pmatrix}^2 = \det \begin{pmatrix} \mathbf{G}^T \mathbf{G} & \mathbf{G}^T \mathbf{y} \\ \mathbf{y}^T \mathbf{G} & \mathbf{y}^T \mathbf{y} \end{pmatrix} = \mathbf{y} \cdot \mathbf{y} \det(\mathbf{G}^T \mathbf{G} - (\mathbf{y} \cdot \mathbf{y})^{-1} \mathbf{G}^T \mathbf{y} \mathbf{y}^T \mathbf{G}). \quad (8.3)$$

Using this and $\mathbf{A}^T \begin{pmatrix} \mathbf{n} \\ \delta_t \end{pmatrix} = 0$ we get

$$\det(\mathbf{A}^T \mathbf{A}) = (1 + \delta_t^2)^{-1} \det \begin{pmatrix} \mathbf{A} & \mathbf{n} \\ & \delta_t \end{pmatrix}^2. \quad (8.4)$$

An elementary calculation yields

$$\det \begin{pmatrix} \mathbf{I} - \delta \mathbf{H} & -\delta \mathbf{n}_t \\ \mathbf{n}^T \delta_t & 1 + \delta_t^2 \end{pmatrix} = (1 + \delta_t^2) \det(\mathbf{I} - \delta \mathbf{H}) = (1 + \delta_t^2) \prod_{i=1}^2 (1 - \delta \kappa_i).$$

Using this we obtain

$$\begin{aligned} \det \begin{pmatrix} \mathbf{A} & \mathbf{n} \\ \delta_t & \delta_t^2 \end{pmatrix} &= \det \begin{pmatrix} \mathbf{I} - \delta \mathbf{H} & -\delta \mathbf{n}_t \\ \delta_t \mathbf{n}^T & 1 + \delta_t^2 \end{pmatrix} \det \left(\begin{pmatrix} \mathbf{P} & -\delta_t \mathbf{n} \\ 0 & 1 \end{pmatrix} \mathbf{F} \quad \mathbf{n}_0 \right) \\ &= (1 + \delta_t^2) \prod_{i=1}^2 (1 - \delta \kappa_i) \det \left(\begin{pmatrix} \mathbf{P} & -\delta_t \mathbf{n} \\ 0 & 1 \end{pmatrix} \mathbf{F} \quad \mathbf{n}_0 \right). \end{aligned} \quad (8.5)$$

We apply (8.3) with $\mathbf{G} = \begin{pmatrix} \mathbf{P} & -\delta_t \mathbf{n} \\ 0 & 1 \end{pmatrix} \mathbf{F}$, which yields

$$\begin{aligned} \det \left(\begin{pmatrix} \mathbf{P} & -\mathbf{n} \delta_t \\ 0 & 1 \end{pmatrix} \mathbf{F} \quad \mathbf{n}_0 \right)^2 &= \det (\mathbf{G}^T \mathbf{G} - \mathbf{G}^T \mathbf{n}_0 \mathbf{n}_0^T \mathbf{G}) = \det \left(\mathbf{G}^T \begin{pmatrix} \mathbf{P} & 0 \\ 0 & 1 \end{pmatrix} \mathbf{G} \right) \\ &= \det \left(\mathbf{F}^T \begin{pmatrix} \mathbf{P} & 0 \\ 0 & 1 \end{pmatrix} \mathbf{F} \right) = \det \left(\boldsymbol{\Sigma}^T \mathbf{U}^T \begin{pmatrix} \mathbf{P} & 0 \\ 0 & 1 \end{pmatrix} \mathbf{U} \boldsymbol{\Sigma} \right). \end{aligned}$$

We define $\mathbf{U}_m := (\mathbf{u}_1, \mathbf{u}_2, \mathbf{u}_3) \in \mathbb{R}^{4 \times 3}$ and $\boldsymbol{\Sigma}_m := \text{diag}(\sigma_1, \sigma_2, \sigma_3) \in \mathbb{R}^{3 \times 3}$, hence, $\mathbf{U} \boldsymbol{\Sigma} = \mathbf{U}_m \boldsymbol{\Sigma}_m$. Thus we get

$$\det \left(\begin{pmatrix} \mathbf{P} & -\mathbf{n} \delta_t \\ 0 & 1 \end{pmatrix} \mathbf{F} \quad \mathbf{n}_0 \right) = \det \left(\mathbf{U}_m^T \begin{pmatrix} \mathbf{P} & 0 \\ 0 & 1 \end{pmatrix} \mathbf{U}_m \right)^{\frac{1}{2}} \prod_{i=1}^3 \sigma_i.$$

Combining this with the results in (8.2), (8.4) and (8.5) we get

$$\mu_h^S = (1 + \delta_t^2)^{\frac{1}{2}} \prod_{i=1}^2 (1 - \delta \kappa_i) \det \left(\mathbf{U}_m^T \begin{pmatrix} \mathbf{P} & 0 \\ 0 & 1 \end{pmatrix} \mathbf{U}_m \right)^{\frac{1}{2}}. \quad (8.6)$$

Now note

$$\det \left(\mathbf{U}_m^T \begin{pmatrix} \mathbf{P} & 0 \\ 0 & 1 \end{pmatrix} \mathbf{U}_m \right) = \det (\mathbf{I} - \mathbf{U}_m^T \mathbf{n}_0 \mathbf{n}_0^T \mathbf{U}_m) = 1 - (\mathbf{U}_m^T \mathbf{n}_0) \cdot (\mathbf{U}_m^T \mathbf{n}_0). \quad (8.7)$$

From $\mathbf{n}_0 = \sum_{i=1}^3 (\mathbf{n}_0 \cdot \mathbf{u}_i) \mathbf{u}_i + (\mathbf{n}_0 \cdot \mathbf{n}_{S_h}) \mathbf{n}_{S_h}$ it follows that

$$1 = \sum_{i=1}^3 (\mathbf{n}_0 \cdot \mathbf{u}_i)^2 + (\mathbf{n}_0 \cdot \mathbf{n}_{S_h})^2 = (\mathbf{U}_m^T \mathbf{n}_0) \cdot (\mathbf{U}_m^T \mathbf{n}_0) + (\mathbf{n}_0 \cdot \mathbf{n}_{S_h})^2.$$

Using this and (8.6)-(8.7) we get

$$\mu_h^S = (1 + \delta_t^2)^{\frac{1}{2}} \prod_{i=1}^2 (1 - \delta \kappa_i) \mathbf{n}_0 \cdot \mathbf{n}_{S_h}$$

Using the identity $\delta_t = -\mathbf{w}^e \cdot \mathbf{n} = V^e$ on S_h^n completes the proof.

REFERENCES

- [1] E. BURMAN, P. HANSBO, M. G. LARSON, AND A. MASSING, *Cut finite element methods for partial differential equations on embedded manifolds of arbitrary codimensions*, ESAIM Math. Model. Numer. Anal., 52 (2018), pp. 2247–2282.
- [2] A. DEMLOW, *Higher-order finite element methods and pointwise error estimates for elliptic problems on surfaces*, SIAM J. Numer. Anal., 47 (2009), pp. 805–827.
- [3] A. DEMLOW AND G. DZIUK, *An adaptive finite element method for the Laplace-Beltrami operator on implicitly defined surfaces*, SIAM J. Numer. Anal., 45 (2007), pp. 421–442.
- [4] G. DZIUK AND C. M. ELLIOTT, *Finite element methods for surface PDEs*, Acta Numer., 22 (2013), pp. 289–396.
- [5] ———, *L^2 -estimates for the evolving surface finite element method*, Math. Comp., 82 (2013), pp. 1–24.
- [6] C. M. ELLIOTT AND C. VENKATARAMAN, *Error analysis for an ALE evolving surface finite element method*, Numerical Methods for Partial Differential Equations, 31 (2015), pp. 459–499.
- [7] J. GRANDE, C. LEHRENFELD, AND A. REUSKEN, *Analysis of a high-order trace finite element method for PDEs on level set surfaces*, SIAM J. Numer. Anal., 56 (2018), pp. 228–255.
- [8] J. GRANDE AND A. REUSKEN, *A higher order finite element method for partial differential equations on surfaces*, SIAM Journal on Numerical Analysis, 54 (2016), pp. 388–414.
- [9] S. GROSS AND A. REUSKEN, *Numerical methods for two-phase incompressible flows*, vol. 40 of Springer Series in Computational Mathematics, Springer-Verlag, Berlin, 2011.
- [10] A. HANSBO, P. HANSBO, AND M. G. LARSON, *A finite element method on composite grids based on Nitsche’s method*, M2AN Math. Model. Numer. Anal., 37 (2003), pp. 495–514.
- [11] F. HEIMANN AND C. LEHRENFELD, *Geometry error analysis of a parametric mapping for higher order unfitted space-time methods*, Preprint arXiv:2311.02348(v3), (2024).
- [12] F. HEIMANN, C. LEHRENFELD, AND J. PREUSS, *Geometrically higher order unfitted space-time methods for PDEs on moving domains*, SIAM J. Sci. Comp., 45 (2023), pp. B139–B165.
- [13] A. J. JAMES AND J. LOWENGRUB, *A surfactant-conserving volume-of-fluid method for interfacial flows with insoluble surfactant*, J. Comput. Phys., 201 (2004), pp. 685–722.
- [14] B. KOVÁCS, *High-order evolving surface finite element method for parabolic problems on evolving surfaces*, IMA J. Numer. Anal., 38 (2018), pp. 430–459.
- [15] B. KOVÁCS, *Numerical surgery for mean curvature flow of surfaces*, arXiv preprint arXiv:2210.14046, (2022).
- [16] C. LEHRENFELD, *High order unfitted finite element methods on level set domains using isoparametric mappings*, Comput. Methods Appl. Mech. Engrg., 300 (2016), pp. 716–733.
- [17] C. LEHRENFELD, M. A. OLSHANSKII, AND X. XU, *A stabilized trace finite element method for partial differential equations on evolving surfaces*, SIAM J. Numer. Anal., 56 (2018), pp. 1643–1672.
- [18] C. LEHRENFELD AND A. REUSKEN, *Analysis of a high-order unfitted finite element method for elliptic interface problems*, IMA J. of Numer. Anal., 38 (2017), pp. 1351–1387.
- [19] M. A. OLSHANSKII AND A. REUSKEN, *Error analysis of a space-time finite element method for solving PDEs on evolving surfaces*, SIAM J. Numer. Anal., 52 (2014), pp. 2092–2120.
- [20] M. A. OLSHANSKII, A. REUSKEN, AND X. XU, *An Eulerian space-time finite element method for diffusion problems on evolving surfaces*, SIAM J. Numer. Anal., 52 (2014), pp. 1354–1377.
- [21] J. PREUSS, *Higher order unfitted isoparametric space-time FEM on moving domains*, master’s thesis, NAM, University of Göttingen, 2018.
- [22] H. SASS, *Space-time Trace Finite Element Methods for Partial Differential Equations on Evolving Surfaces*, PhD thesis, RWTH Aachen University, 2022.
- [23] H. SASS AND A. REUSKEN, *An accurate and robust Eulerian finite element method for partial differential equations on evolving surfaces*, Computers & Mathematics with Applications, 146 (2023), pp. 253–270.
- [24] V. THOMEE, *Galerkin finite element methods for parabolic problems*, Springer, Berlin, 1997.
- [25] Q. ZHAO, W. JIANG, AND W. BAO, *A parametric finite element method for solid-state dewetting problems in three dimensions*, SIAM J. Sci. Comput., 42 (2020), pp. B327–B352.